

1 **Comprehensive Automobile Research System (CARS) – a**

2 **Python-based Automobile Emissions Inventory Model**

3 Bok H. Baek¹, Rizzieri Pedruzzi², Minwoo Park³, Chi-Tsan Wang¹, Younha Kim³, Chul-Han
4 Song⁴, and Jung-Hun Woo³

5 ¹Center for Spatial Information Science and Systems – George Mason University, Fairfax, VA, USA.

6 ²Department of Sanitary and Environmental Engineering, Federal University of Minas Gerais, Belo Horizonte,
7 Brazil.

8 ³Department of Advanced Technology Fusion, Konkuk University, Republic of Korea

9 ⁴School of Earth and Environmental Engineering, Gwangju Institute Science and Technology, Republic of Korea

10 *corresponding to: Jung-Hun Woo (jwoo@konkuk.ac.kr)*

11 **Abstract**

12 The Comprehensive Automobile Research System (CARS) is an open-source python-based
13 automobile emissions inventory model designed to efficiently estimate high quality emissions
14 from motor-vehicle emission sources. It can estimate the criteria air pollutants, greenhouse gases,
15 and air toxics in various temporal resolutions at the national, state, county, and any spatial
16 resolution based on the spatiotemporal resolutions of input datasets. The CARS is designed to
17 utilize the local vehicle activity data, such as vehicle travel distance, road link-level network
18 Geographic Information System (GIS) information, and vehicle-specific average speed by road
19 type, to generate a temporally and spatially resolved automobile emissions inventory for
20 policymakers, stakeholders, and the air quality modeling community. The CARS model adopted
21 the European Environment Agency’s (EEA) onroad automobile emissions calculation
22 methodologies to estimate the hot exhaust, cold start, and evaporative emissions from onroad
23 automobile sources. It can optionally utilize average speed distribution (ASD) of all road types to
24 reflect more realistic vehicle speed variations. Also, utilizing high-resolution road GIS data allows
25 the CARS to estimate the road link-level emissions to improve the inventory's spatial resolution.
26 When we compared the official 2015 national mobile emissions from Korea’s Clean Air Policy
27 Support System (CAPSS) against the ones estimated by the CARS, there is a moderate increase of
28 volatile organic compounds (VOCs) (33%), carbon monoxide (CO) (52%), and fine particulate
29 matter (PM_{2.5}) (15%) emissions while nitrogen oxides (NO_x) and sulfur oxides (SO_x) are reduced
30 by 24% and 17% in the CARS estimates. The main differences are driven by the usage of different
31 vehicle activities and the incorporation of road-specific ASD, which plays a critical role in hot
32

33 exhaust emission estimates but wasn't implemented in Korea's CAPSS mobile emissions
34 inventory. While 52% of vehicles use gasoline fuel and 35% use diesel, gasoline vehicles only
35 contribute 7.7% of total NO_x emissions while diesel vehicles contribute 85.3%. But for VOC
36 emissions, gasoline vehicles contribute 52.1% while diesel vehicles are limited to 23%. While
37 diesel buses are only 0.3% of vehicles, each vehicle has the largest contribution to NO_x emissions
38 (8.51% of NO_x total) due to it having longest daily vehicle kilometer travel (VKT). In VOC
39 emission part, CNG buses are the largest contributor with 19.5% of total VOC emissions. For
40 primary PM_{2.5}, more than 98.5% is from diesel vehicles. The CARS model's in-depth analysis
41 feature can assist government policymakers and stakeholders develop the best emission abatement
42 strategies.

43 Keywords: inventory: automobile, vehicle emissions, hot exhaust, cold start, evaporative, python

44 **1 Introduction**

45 Globally, ambient pollution causes more than 4.2 million premature deaths every year
46 (Cohen et al., 2017), and Burnett et al. estimate the health burden is closer to 9 million deaths from
47 ambient PM concentrations (Burnett et al., 2018). To effectively mitigate air pollutants, both
48 developed and developing countries' governments have been implementing stringent air pollution
49 abatement control policies to reduce harmful regional air pollutants (Hogrefe et al., 2001a; Hogrefe
50 et al., 2001b; Dennis et al., 2010; Rao et al., 2011; Appel et al., 2013; Luo et al., 2019). The CTM
51 simulation results strongly rely on precise input data, such as emission inventory, meteorology,
52 land surface parameters, and chemical mechanisms in the atmosphere.

53 The transportation emission sector is one of the major anthropogenic emissions in urban
54 areas. The tailpipe emissions from the vehicle's combustion process contain many air pollutants,
55 including nitrogen oxides (NO_x), volatile organic compounds (VOCs), carbon monoxide (CO),
56 ammonia (NH₃), sulfur dioxide (SO₂), and primary particulate matter (PM) which will participate
57 in the formation of detrimental secondary pollutants like ozone and PM_{2.5} in the atmosphere. In
58 the Seoul Metropolitan Area (SMA) in South Korea, transportation automobile sources contribute
59 the most to the total NO_x and primary PM_{2.5} emissions across all emission sources. (Choi et al.,
60 2014; Kim et al., 2017a; Kim et al., 2017b; Kim et al., 2017c). Thus, it is critical to understand and
61 represent better on the emission patterns from the transportation automobile sources in the CTM
62 model. The use of process-based automobile emission models is highly recommended to meet the
63 needs in CTM model because it can estimate the highly resolved spatiotemporal automobile
64 emissions. (Moussiopoulos et al., 2009; Russell and Dennis, 2000).

65 There are two methodologies known in emission inventory development: top-down and
66 bottom-up. The choice of methods is determined by the input data availability. The top-down
67 approach primarily relies on the aggregated and generalized country or regional information,

68 especially in developing countries where only limited datasets and information are available. It has
69 its limitations on representing the vehicle emission process realistically due to the lack of detailed
70 activity and ancillary supporting data. However, the bottom-up approach requires higher-quality
71 spatiotemporal activity datasets like road network information, vehicle composition (vehicle type,
72 engine size, vehicle age, and fuel-technology), pollutant-specific emissions factors, road segment
73 length, traffic activity data, and fuel consumption (EEA, 2019; Ibarra-Espinosa et al., 2018b;
74 IEMA, 2017). It can generate more accurate and detailed automobile emissions across various
75 operating processes, such as hot exhaust, evaporative, idling, and hot soak (Nagpure et al., 2016;
76 Ibarra-Espinosa et al., 2018a).

77 There are several bottom-up mobile emissions models available, like MOVES (MOtor
78 Vehicle Emissions Simulator) from the U.S. Environmental Protection Agency (USEPA), the
79 European Environment Agency's (EEA) model COPERT (COmputer Programmed to calculate
80 Emissions from Road Transport), the HERMES (High-Elective Resolution Modelling Emission
81 System) from Barcelona Supercomputing Center (Guevara et al., 2019), the VEIN (Vehicular
82 Emissions INventory) model developed by Ibarra-Espinosa et al. (2017), and the VAPI (Vehicular
83 Air Pollution Inventory) model developed by Nagpure and Gurjar (2012) for India (Nagpure et al.,
84 2016). While these models are all bottom-up emission inventory models, a single model cannot
85 meet all modelers, policymakers, and stakeholders' needs because each model holds its own pros
86 and cons. They are developed differently to meet specific user needs based on the types of traffic
87 activity and emission factors, emission calculation methodologies, and other optional/available
88 traffic-related inputs such as average speed distribution and geographical resolution. Each model
89 is developed with different levels of specificity, underlying data set and modeling assumptions.

90 The MOVES model has the strength to generate high-quality emissions for up to 16
91 different emission processes (i.e., Running Exhaust, Start Exhaust, Evaporative, Refueling,
92 Extended Idling, Brake, Tire, etc.). It can simulate not only county-level but also road segment
93 level depending on data availability. It can also reflect local meteorological conditions, such as
94 ambient temperature and relative humidity, which can significantly impact both pollutants and
95 emissions processes (Choi et al., 2017; Perugu et al., 2018). Disadvantage of this model is it
96 difficult to update and apply to countries outside of the U.S. because MOVES model is high degree
97 of specificity. The COPERT model that is widely used in European countries has its advantages,
98 such as the capability to model emissions in high resolution. Additionally, it is fully integrated
99 with the EEA's onroad vehicle emissions factors guidelines and can generate a complete quality
100 assurance (QA) and visualization summary (Ntziachristos et al., 2009). The cons are that it is a
101 proprietary commercial licensed software, limited to EEA guidance, and challenging to modify
102 and update with any key input datasets like the latest emission factors from non-European
103 countries (Lejri et al., 2018; Rey DR, 2021; Li et al., 2019; Lv et al., 2019; Smit et al., 2019).

104 The HERMES and VEIN are both recently released bottom-up inventory models. They
105 have their pros in that they are both open-source models based on open-source computing

106 languages (Python and R), which provide transparency of emission calculations with a
107 considerable amount of data behind it (Ibarra-Espinosa et al., 2018b; Guevara et al., 2019). Both
108 models are driven by comma-separated value (CSV) formatted input files, making it very easy for
109 users to modify the input datasets. They are also based on the EEA's emission calculation method
110 and equipped with a complete QA and visualization tool based on Python and R libraries. However,
111 it is not an easy task to update the emission factors, and generate other required input datasets for
112 other countries, and lacks support for any control strategy plan feature to generate a responsive
113 reduced emissions inventory for policymakers, stakeholders, and modelers.

114 The VAPI (Vehicular Air Pollution Inventory) model was developed in India because the
115 country does not have an extensive and robust traffic-related dataset to run these kinds of vehicular
116 emissions inventory models (Nagpure et al., 2016; Perugu, 2019).

117 There are also a few shortcomings of incorporating these bottom-up models into CTM
118 studies. These models require strong programming skills to operate, such as collecting and
119 preparing the input data to fit the model requirement, configuring the model variables, and
120 changing specific variables that may be embedded in the code. Another downside is that while the
121 administration-level emissions inventory can be estimated by those models, it requires a 3rd party
122 emissions processor like the SMOKE (Sparse Matrix Operator Kerner Emissions) modeling
123 system (Baek and Seppanen, 2021) to process and generate spatially and temporally resolved
124 emissions inputs for CTM. Some detailed information, like link-level hourly driving patterns, can
125 be lost in the emissions processing steps.

126 There is no single model capable of meeting all the requirements across various spatial and
127 temporal scales (Pinto et al., 2020). However, transparency, simplicity, and a user-friendly
128 interface are requirements for those who mainly work in transportation policy and air quality
129 modeling development (Fallahshorshani et al., 2012; Kaewunruen et al., 2016; Sallis et al., 2016;
130 Sun et al., 2016; Tominaga and Stathopoulos, 2016). Thus, the ideal mobile emissions modeling
131 system would be computationally optimized, easy-to-use, and have a user-friendly interface.
132 Additionally, the model should easily adapt detailed local activity information and the state-of-art
133 emission factors as an input to represent them in the highest resolution possible in time and space.

134 We have developed the Comprehensive Automobile Research System (CARS) to meet these
135 requirements, especially for the air quality research community, policymakers, and air quality
136 modelers. The CARS is a stand-alone, fully modularized, computationally optimized, python-
137 based automobile emission model. The modularization improves the efficiency of processing times.
138 Once district and road link-level annual/monthly/daily total emissions are computed, the rest of
139 the processes are optional. It can generate chemically speciated, spatially gridded hourly emissions
140 for CTMs without any 3rd party emissions modeling system to develop the highest quality CTM-
141 ready emissions inputs. All functions are operated by independent modules and can be enabled by
142 users. Details on modularization will be discussed later. The CARS model can be easily adopted

143 and is simple for users to add new functions or modules in the future. The application of the CARS
144 to South Korea will be described in detail later.

145 **2 CARS Emissions Calculation**

146 The CARS is an open-source Python-based customizable motor vehicle emissions
147 processor that estimates onroad and offroad emissions for specific criteria and toxic air pollutants.
148 Figure 1 is a schematic of the CARS overview. It applies vehicle, engine, and fuel specific
149 emission factors to traffic data to estimate the local level annual, monthly, and daily total emissions
150 inventory. The emissions inventory calculations require the list of pollutant-specific emissions
151 factors by vehicle age, local activity data, average speed profile/distribution by road type, and
152 geographic information system (GIS) road segment shapefiles inputs. The spatial resolution of
153 vehicle kilometer travel (VKT) defines the CARS geographic scale (i.e. district, county, state, and
154 country) for emission calculations. Unlike the district-level Korea Clean Air Policy Support
155 System (CAPSS) automobile emission inventory (Lee et al., 2011a; Lee et al., 2011b), the CARS
156 applies high-resolution annual average daily traffic (AADT) data from the road GIS shapefiles to
157 distribute the total district emissions into road link-level emissions. Optionally, these road link-
158 level emissions can be used to generate spatially gridded CTM-ready emissions input data once
159 the output modeling domain is defined. The summary of input files by categories are presented in
160 Appendix H. How the CARS estimates spatially and temporally enhanced automobile emissions
161 inventories will be discussed in detail next chapter.

162 South Korean traffic databases from the Korea CAPSS team (Lee et al., 2011b) from the
163 National Institute of Environmental Research (NIER) were used in this study to compute the
164 updated onroad automobile emissions inventory. The databases include individual vehicle activity
165 data (daily total VKT), road activity data (average speed distribution by road), vehicle age specific
166 emission factors, road type information, surface weather data, and GIS road shapefiles.

167 **2.1 Individual Daily Average VKT Activity Data**

168 The individual vehicle VKT data is used to reflect the human activity. This study imported
169 the national registered vehicle-specific daily total VKT from South Korea's Vehicle Inspection
170 Management System (VIMS), which belongs to the Korea Transportation Safety Authority
171 (KTSA). It contains over 50 million records from 2013 to 2017. For the CARS model, we first
172 sorted these records by the vehicle identification number (VIN) to remove any duplicates and then
173 built vehicle-specific daily total VKT traffic activity data in the CSV format. The summary of
174 those vehicle numbers and VKTs is presented in Fig. 2. Sedan vehicles using gasoline fuel
175 comprise the greatest percentage of total vehicles at 47% (~10.4 million) and have the highest
176 VKT. Most vehicles demonstrate similar patterns between the number of vehicles and daily VKT.

177 However, as expected, LPG (liquefied petroleum gas)-fueled taxi are high in VKT compared to
178 the number of vehicles due to their daily long distance travel pattern.

179 The VIN (*vin*) information is used to calculate vehicle-specific daily average VKT (VKT_{vin} ,
180 km d⁻¹). In Eq. (1), the individual daily average vehicle VKT (VKT_{vin}) is calculated based on the
181 cumulative mileage ($M_{f;vin}$) between the last inspection date ($D_{f;vin}$) and registration date ($D_{0;vin}$).
182 Each vehicle is categorized with Korea's NIER defines the vehicle types (Ryu et al., 2003; Ryu et
183 al., 2004; Ryu et al., 2005; Lee et al., 2011a) that based on a combination of vehicle types (e.g.,
184 sedan, truck, bus, etc), engine sizes (e.g., compact, full size, midsize, etc) and fuel types (e.g.,
185 gasoline, diesel, LPG, etc). Full details of vehicle types and daily total VKT are shown in Appendix
186 A and B.

$$187 \quad VKT_{vin} = \frac{M_{f;vin}}{D_{f;vin} - D_{0;vin}} \quad (1)$$

188 2.2 Emission Calculations

189 Automobile emission sources include motorized engine sources on the paved road network
190 including off-network (e.g., drive way and parking lots). The CARS model doesn't simulate
191 emissions from nonroad emission sources, such as aviation, railways, construction, agricultures,
192 lawn mower, and boats yet. The CARS model simulates the onroad automobile emissions from
193 network roads using their local traffic-related datasets. The following section explains the
194 approach of the onroad automobile emission processes. The onroad emission (E_{onroad}) in the CARS
195 is defined in Eq. (2), which includes three major emission processes (Ntziachristos and Samaras,
196 2000):

$$197 \quad E_{onroad} = E_{hot} + E_{cold} + E_{vap} \quad (2)$$

198 The hot exhaust emissions (E_{hot}) are the vehicle's tailpipe emissions when the internal combustion
199 engine (ICE) combusts the fuel to generate energy under the average operating temperature. The
200 cold start emissions (E_{cold}) are the tailpipe emissions from the ICE when the cold vehicle engine is
201 ignited and the operational temperature is below average condition. The evaporative VOC
202 emissions (E_{vap}) are the emissions evaporated/permeated from the fuel systems (fuel tanks,
203 injection systems, and fuel lines) of vehicles.

204 The CARS first applies the hot exhaust emission factors by vehicle type, age, fuel, engine,
205 and pollutants to individual daily total VKT to compute the hot exhaust emissions. The rest of the
206 processes for cold start and evaporative emissions are calculated afterwards. The emission
207 calculation methodologies used in the CARS model are based on tier 2 and tier 3 methodologies
208 from the EEA's mobile emission inventory guidebook (EEA, 2019) to be consistent with Korea's
209 National Emission Inventory System (NEIS) (Lee et al., 2011a).

2.2.1 Hot Exhaust Emissions

Hot exhaust emissions, which is from the vehicle's tailpipe, is the exhaust gas from the combustion process in an ICE. The ICE combustion cycle generally causes incomplete combustion processes which emit hydrocarbons, carbon monoxide (CO), and particulate matter (PM) which not completely controlled from the aftertreatment equipment, such as three-way catalytic converter and released into the atmosphere. The sulfur compounds in the fuel are oxidized and become sulfur oxides (SO_x). Nitrogen oxides (NO_x) are produced during the combustion process due to the abundant nitrogen (N₂) and oxygen (O₂) in the atmosphere.

Equation 3 represents the calculation of daily individual vehicle hot exhaust emission rate, $E_{hot;p,vin,myr}$ (g d⁻¹) of pollutant (p). An individual vehicle-specific daily VKT_{vin} (km d⁻¹) is estimated by Eq. (1). The $EF_{hot;p,v,myr,s}$ (g/km) is the hot exhaust emission factor of pollutants (p) for the vehicle type (v), vehicle manufacture year (myr), and average vehicle speed (s). The district's total emission rate is the total hot exhaust emissions from all individual vehicles within the same district.

$$E_{hot;p,vin,myr} = DF_{p,v,myr} \times VKT_{vin} \times EF_{hot;p,v,myr,s} \quad (3)$$

The deterioration factor (DF) in Eq. (3) is an optional function in the CARS. The deterioration process is caused by vehicle aging and can lead to the increase of vehicle emissions. The vehicle DF is varied by vehicle type (v), pollutant (p), and vehicle manufacture year (myr). The CARS model computes vehicle ages based on the vehicle manufacture year and model simulation year. According to the guidance of deterioration factors calculation from NIER, there is no deterioration in a new vehicle during their first five years. After five years, the deterioration factors can increase the 5~10% range depending on the type of vehicle and pollutants. Deterioration processes can cause up to 100% increase of emissions in fifteen-year-old vehicles. Currently, the DF is an empirical coefficient that varies by vehicle age (Lee et al., 2011a).

The hot exhaust emission factor, $EF_{hot;p,v,s}$ (g/km) is a function of vehicle speed (s) with other empirical coefficients: a, b, c, d, f, k . The emission factor formula and those coefficients were developed by NIER CAPSS (Lee et al., 2011a). These coefficients are varied by pollutants (p), vehicle type (v), vehicle manufacture year (myr), and vehicle speed (s). The vehicle speed affects the combustion efficiency of an ICE and impacts the emission rates and its composition from the tailpipe.

$$EF_{hot;p,v,myr,s} = k(a \times s^b + c \times s^d + f) \quad (4)$$

While vehicle speed plays a critical role in hot exhaust emissions from most vehicles, NO_x emissions from some diesel vehicles show sensitivity to local ambient temperature along with vehicle speed (Ntziachristos and Samaras, 2000). Figure 3 shows the dependency of NO_x emission factors from compact diesel vehicles to vehicle speed (Fig. 3a) and ambient temperature (Fig. 3b).

244 Figure 3a shows a significant decrease of NO_x emissions while speed increases between 0 and 70
245 km. Figure 3b demonstrates the significance of local meteorology on NO_x emissions from a
246 compact diesel sedan. Based on these NIER's CAPSS emission factors, the sensitivity to local
247 ambient temperature is limited to NO_x pollutant emissions from diesel vehicles.

248 Due to its high sensitivity to the vehicle operating speed, it is important for the CARS to
249 simulate realistic speed patterns for accurate emissions estimates. When a single speed is assigned
250 to compute hot exhaust emissions, it won't reflect the emissions under low-speed circumstances.
251 To overcome this limitation, the CARS has adopted the 16 average speed bins concepts for a better
252 representation of vehicle speed distribution that varies by road type (i.e., local, highway,
253 expressway). We have implemented a feature for the CARS optionally to apply road-specific
254 average speed distributions (ASD) ($A_{bin,r}$), which represents the fractions of 16-speed bins (*bin*)
255 (from 0 to 121 km h⁻¹ defined in Appendix E) for eight different road types (*r*) (No.101-108, shown
256 in Appendix C) as classified by CAPSS (Fig. 4a). Although ASD patterns vary by region and time,
257 current CARS model version does not support ASD application by region and time of day due to
258 the lack of region and time dependent ASD availability in South Korea.

259 We first developed the ASD (Fig. 4a) for eight different road types (No. 101-108) in South
260 Korea based on the latest road link-specific average speed and the length of link from the SK GIS
261 road network shapefiles (NIER, 2018). Because the original link-level speed data is averaged, we
262 used the link length as a weighting factor to show the variation of speed pattern for each link.
263 However, the ASD based on the SK GIS road shapefiles wasn't able to capture the low-speed
264 range (<16 km h⁻¹) that occurs while it operates (Fig. 4a). It caused the significant underestimation
265 of NO_x and VOC emissions compared to the CAPSS (Appendix G).

266 To address this SK ASD issue, we incorporated the ASD (Figure 4b) from the state of
267 Georgia developed by U.S. EPA to improve the representation of the low-speed ranges (speed bin
268 #1 and #2 for road type 1 to 7). We increased the total fractions of low-speed bins (the 2:1 ratio of
269 fractions of bin #1 and #2) by 2% for interstate expressways, 3% for urban expressways, 7% for
270 all highways, and 15% for all local roads. The increases in low-speed bins lowered the distributions
271 of other higher speed bins homogeneously due to the renormalization of fractions by road type.
272 Figure 4c shows the renormalized hybrid-ASDs of all road types based on SK ASD and Georgia
273 ASD. We understand, the hybrid-ASD approach is not ideal for SK onroad emission inventory
274 development. However, it clearly demonstrates the CARS's capability and sensitivity to the
275 vehicle speed representation and the impacts of ASD to the local onroad mobile inventories.

276 While 16-speed bins ASD application is critical to computing more realistic hot exhaust
277 emissions, there should be some restrictions on certain road types. Users can adjust the restricted
278 roads control table input file to limit the vehicle types that can only be operated on a particular
279 road type. For example, motorcycles are limited to local roads (No. 104, 106, and 107), but not on
280 expressways (No. 101, 102, 103, 105, and 108) due to its traffic regulation rules. Heavy trucks are

281 only allowed on the highway (No. 101, 102, 103, 105, and 108.) by law. The details of the road
 282 restriction control table format can be found on the CARS's user's guide from the CARS Github
 283 website (https://github.com/bokhaeng/CARS/tree/master/docs/User_Manual).

284 The 16-speed bins averaged speed distribution calculated by road type ($A_{bin,r}$) and road type
 285 weight factors ($\omega_{r,d}$) in a district (d) from Eq. (13) are added to the CARS hot exhaust emissions
 286 equation (Eq. 3). The hot exhaust emissions from individual vehicles ($E_{hot;p,vin,myr}$) can be
 287 calculated by considering road-specific speed bins distribution (Eq. 5). Although the vehicles may
 288 be operated in different districts from their registered district, this is our best method to estimate
 289 the vehicle speed for hot exhaust emissions.

$$290 \quad E_{hot;p,vin,myr} = DF_{p,v,myr} \times \sum_{bin} (VKT_{vin} \times EF_{hot;p,v,myr,s} \times A_{bin,r}) \quad (5)$$

291 2.2.2 Cold Start Emissions

292 The cold start emissions occur when a cold-engine vehicle is ignited. The lower
 293 temperature of the ICE is not an optimal condition for complete fuel combustion. This process
 294 lowers the combustion efficiency (CE) and increases the emissions of hydrocarbon and CO
 295 pollutants from the tailpipe exhaust (Jang et al., 2007). The CARS can estimate the cold start
 296 emissions for vehicles using gasoline, diesel, or liquefied petroleum gas (LPG) fuel. Besides the
 297 vehicle and engine type, road type also plays a critical role in the quantity of cold start emissions
 298 because it occurs mostly in parking lots and rarely on highways.

299 The cold start emission, E_{cold} (g d⁻¹), is derived from the hot exhaust emissions, the ratio of
 300 hot to cold exhaust emissions ($EF_{cold}/EF_{hot} - 1.0$), and the percentage of the traveled distance with
 301 a cold engine (Eq. 6).

$$302 \quad E_{cold;p,v} = \beta_T \times E_{hot;p,v} \times \left(\frac{EF_{cold;p,v}}{EF_{hot;p,v}} - 1.0 \right) \quad (6)$$

303 The emission factor of cold start emissions (EF_{cold}) is not directly calculated from
 304 measurement data like hot exhaust emissions ($E_{hot;p,v}$), but measured under different ambient
 305 temperatures (T). The CARS model applies linear regression models developed by CAPSS to
 306 estimate the increasing ratio of cold start to hot exhaust emissions (EF_{cold}/EF_{hot}) under different
 307 temperatures (T) (Eq. 7). In this equation, A and B are the empirical coefficients that vary by the
 308 pollutants (p) and vehicle type (v).

$$309 \quad \left(\frac{EF_{cold;p,v}}{EF_{hot;p,v}} \right) = A_{p,v} + B_{p,v} \times T \quad (7)$$

310 β is the percentage of the distance traveled under a cold engine. It also depends on the
 311 ambient temperature. Cold ambient temperatures cause a longer distance traveled under a cold

312 engine due to the slower heating time. According to the CAPSS database for Seoul city (Lee et al.,
 313 2011a), the empirical linear equation for β is shown in Eq. (8). This formula represents how
 314 ambient temperature affects β . For example, when the average temperature is -2°C , β is 34.8%.
 315 In summer, the monthly average temperature is 25.7°C , which causes β to drop to 21%.

$$316 \quad \beta = 0.647 - 0.025 \times 12.35 - (0.00974 - 0.000385 \times 12.35) \times T \quad (8)$$

317 **2.2.3 Evaporative VOC Emissions**

318 Evaporative emissions are emissions from vehicle fuel that are evaporated into the
 319 atmosphere. This occurs in the fueling system inside the vehicle, such as fuel-tanks, injection
 320 systems, and fuel lines. Diesel vehicles, however, can be exempted due to diesel fuel's low vapor
 321 pressure. The primary sources of evaporative emissions are breathing losses through tank vents
 322 and fuel permeation/leakage. The CARS model adopted the EEA's emission inventory guidebook
 323 (EEA, 2019) to account for three mechanisms to estimate the evaporative VOC emissions (E_{vap}):
 324 diurnal emissions from the tank (e_d), hot and warm soak emissions by fuel injection type (S_{fi}), and
 325 running loss emissions (R) (Eq. 9). Unlike CAPSS, there is a conversion factor (0.075) applied to
 326 E_{vap} for motorcycles to prevent an over-estimation of VOC.

$$327 \quad E_{vap;p,v} = (e_{d;p,v} + S_{fi;p,v} + R_{l;p,v}) \quad (9)$$

328 Diurnal emissions, e_d (g d^{-1}), during the daytime are caused by the ambient temperature
 329 increase and the expansion of fuel vapors inside the fuel tank. Most of the current fuel tank systems
 330 have emission control systems to limit this kind of evaporative VOC emissions. The e_d can be
 331 calculated with the empirical Eq. (10), which was developed by CAPSS. T_l is the monthly average
 332 of the daily lowest temperatures and T_h is the monthly average of the daily highest temperatures.
 333 The empirical coefficient α is 0.2, which represents how 80% of emissions are eliminated by the
 334 vehicle emission control system.

$$335 \quad e_d = \alpha \times 9.1 \exp[0.3286 + 0.0574 \times (T_l) + 0.0614 \times (T_h - T_l - 11.7)] \quad (10)$$

336 Soak emissions (S_{fi}) occur when a hot ICE is turned off; the remaining heat from the ICE
 337 can increase the fuel temperature in the system. The carburetor float bowls are the major source of
 338 the soak emissions. Newer vehicles with fuel injection and return-less fuel systems do not emit
 339 soak emissions. Because most of the current vehicles in South Korea have a new fuel system, soak
 340 emissions (S_{fi}) in the CARS model are set to 0.

341 The running loss emissions (R_l) are from vapors generated in the fuel tank when a vehicle
 342 is in operation (Eq. 11). In some older vehicles, the carburetor and engine operation can increase
 343 the temperature in the fuel tank and carburetor, which can cause a significant increase in
 344 evaporative VOC emissions. VOC emissions from running loss can be greatly increased during

345 warmer weather. However, newer vehicles with fuel injection and return-less fuel systems are not
 346 affected by the ambient temperature. Because most vehicles in South Korea do not use carburetor
 347 technology, we expect running loss emissions to have the least impact (Lee et al., 2011b).

$$348 \quad R_l = \alpha \times L_{r,v} \times [(1 - \beta) \times R_h + \beta \times R_w] \quad (11)$$

349 The empirical coefficient α is 0.1 here, which represents that 90% of the running loss is
 350 avoided by the newer fuel system. L is the distance traveled (km) by road and is the same one used
 351 in hot exhaust emission calculations. β is the same parameter from Eq. (8). The R_h and R_w are the
 352 average emission factors from running loss under hot and warm/cold conditions, respectively.

353 2.3 Road Link-Level Emissions Calculations

354 In general, district-level automobile emissions calculations are driven by district-level
 355 averaged vehicle activity and operating data, which do not reflect realistic spatial patterns of
 356 onroad automobile emissions. The CARS model introduces road link-specific traffic data by
 357 default to develop spatially enhanced road link-specific emissions that reflect more representative
 358 emissions by road link. This high-resolution traffic data is a GIS shapefile that is composed of
 359 many connected segments, which are called “road links.” All road links hold information such as
 360 start/end location coordinates, AADT, road link length, averaged vehicle speed, and road type (No.
 361 101-108).

362 The CARS model applies link-level AADT ($AADT_{d,r,l}$, d^{-1}) and road length ($L_{d,r,l}$) to
 363 compute the road link-specific VKT ($VKT_{d,r,l}$, $km\ d^{-1}$) in Eq. (12). The road links are identified by
 364 district (d), road type (r), and link (l) labels. The road VKT is a parameter that reflects the traffic
 365 activity of each road link and it is different from individual daily vehicle activity data ($VKT_{v,age}$)
 366 in Eq. (1).

$$367 \quad VKT_{d,r,l} = AADT_{d,r,l} \times L_{d,r,l} \quad (12)$$

368 Road link-specific VKT ($VKT_{d,r,l}$) is used to redistribute the district total emissions (E_{onroad})
 369 from Eq. 2 into road link-level emissions. The following three weight factors are computed: the
 370 district weight factors, ω_d (Eq. 13), the road type weight factors, $\omega_{d,r}$ (Eq. 14), and the road-link
 371 weight factors, $\omega_{d,l}$ (Eq. 15). The weight district factors (ω_d) are the renormalization of each
 372 district's total VKT over state-level total VKT (N is the number of districts). The main reason we
 373 performed the renormalization over state-level total VKT is to reflect daily traffic patterns from
 374 multiple districts under the assumption that most vehicles travel within the same state. The road
 375 type weight factors by district ($\omega_{r,d}$) are used to compute road-specific emissions, while road-
 376 specific averaged speed distributions (ASD; $A_{s,r}$) from Eq. (5) are applied to capture vehicle

377 operating speeds by road type. The road link weight factors ($\omega_{d,l}$) are then applied to redistribute
378 the district emissions into road link-level emissions.

379

$$380 \quad \omega_d = \frac{\sum_r \sum_l VKT_{d,r,l}}{\frac{1}{N} \sum_d \sum_r \sum_l VKT_{d,r,l}} \quad (13)$$

$$381 \quad \omega_{d,r} = \frac{\sum_l VKT_{d,r,l}}{\sum_r \sum_l VKT_{d,r,l}} \quad (14)$$

$$382 \quad \omega_{d,l} = \frac{VK T_{d,r,l}}{\sum_r \sum_l VK T_{d,r,l}} \quad (15)$$

383 **3 CARS Configuration**

384 The CARS model is an open-source program based on Python (Guido van Rossum, 2009)
385 that allows the users to efficiently apply open-source modules to develop programs. Users can
386 easily install Python development tools and load customized packages and modules to set up the
387 CARS development environment. All CARS modules are developed using Python v3.6. Other than
388 the GIS road shapefiles, all input files are based in the ASCII CSV format, which can be easily
389 handled by both spreadsheet programs and programming languages, making it more accessible for
390 users of all skillsets. The CARS can not only estimate district-level and spatially enhanced road
391 link-level emissions, but can also generate hourly chemically speciated gridded emissions for
392 CTMs. In addition, the CARS also generates various summary reports, graphics, and
393 georeferenced plots for quality assurance.

394 The required Python modules for the CARS are: “*geopandas*,” “*shapely.geometry*,” and
395 “*csv*” modules to read the shapefiles and table data files. The “*NumPy*” and “*pandas*” modules
396 are used to operate the memory arrays and scientific calculations while the “*pyproj*” module deals
397 with converting the projection coordinate systems. “*matplotlib*” is for generating any type of
398 figures/plots. Furthermore, the CARS model can also read and write Climate and Forecast (CF)-
399 compliant NetCDF-formatted files using “*NetCDF4*”.

400 The first process in the CARS is “*Loading_function_path*”; it allows users to define and
401 check the input file paths. Once all input files are checked, there are six process modules in CARS
402 to process inputs, compute emissions, and generate various output files, including QA reports.
403 Figure 5 is the schematic of the CARS that consists of six process modules with various functions.
404 The six process modules are (1) “**Process activity data**”, (2) “**Process emission factors**”, (3)
405 “**Process shapefile**”, (4) “**Calculate district emissions**”, (5) “**Grid4AQM**”, and (6) “**Plot figures**”.
406 The main purpose of modularizing the CARS is to meet the needs of various communities, such
407 as policymakers, stakeholders, and air quality modelers. While modules (1) through (4) are
408 required to develop the district-level and road link-level emissions inventories, module (5)

409 “**Grid4AQM**” is optional depending on if users want to develop chemically-speciated gridded
410 hourly emissions for CTMs. Also, the modularity system in the CARS allows users to bypass
411 certain modules if it has been previously processed without any changes. For example, if there is
412 no change in traffic activity, emission factors table, or GIS shapefiles, users do not need to run
413 these modules and can simply read the data frame outputs and then run “**Grid4AQM**” for the
414 modeling dates and domain. The “**Grid4AQM**” module will not only improve the computational
415 time for CTMs but also eliminate the need for a 3rd party emissions modeling system like SMOKE
416 (Baek and Seppanen, 2021).

417 The rectangle boxes in Fig. 5 represent the data array and the boxes with rounded edges are
418 the functions in the CARS. Details on the CARS code, input table format, and functions setup
419 information can be found on the CARS GitHub website (Pedruzzi *et al.*, 2020).

420 The “**Process activity data**” module first reads the vehicle activity data, such as an
421 individual vehicle's daily total VKT based on its registered district. The “**Process emission factors**”
422 module reads and stores the emission factors table that holds all pollutant emission factors to
423 estimate the emissions for all vehicles. Meteorology-sensitive emission factors are only limited to
424 NO_x pollutants. District boundary GIS shapefiles and road network shapefiles are processed
425 through “**Process shape file**” to generate the VKT-based redistribution weighting factors from Eq.
426 (13), (14) and (15) for the “**Calculate district emissions**” module to compute district-level and
427 road link-level emission rates (metric tons per year, t yr⁻¹).

428 The redistributed emission rates (t yr⁻¹) from the “**Calculate district emissions**” module
429 present annual total emission rates until district-level VKTs from the “**Process activity data**”
430 module are added. Then, the “**Grid4AQM**” module can generate CTM-ready chemically speciated
431 emissions. The “*Read_chemical*” function from the “**Grid4AQM**” module is designed to process
432 the chemical speciation profile that can convert the inventory pollutants such as CO, NO_x, SO₂,
433 PM₁₀, PM_{2.5}, VOC, and NH₃, into the chemically lumped model species that CTM requires for
434 chemical mechanisms, such as SAPRC (L. and Heo, 2012) and Carbon Bond version 6 (CB6)
435 (Yarwood and Jung, 2010). The “*Read_temporal*” function processes the complete set of monthly,
436 weekly, and hourly temporal allocation profiles that can convert annual total emissions to hourly
437 emissions. “*Read_griddesc*” defines the CTM-ready modeling domain and computes the gridding
438 fractions for all road link-level emissions by overlaying the modeling domain over the GIS
439 shapefiles. Once annual total emissions are chemically speciated, spatially gridded, and temporally
440 allocated into hourly emissions, the “*Gridded_emis*” function will combine emission source-level
441 conversion fractions from each function (*Read_chemical*, *Read_temporal*, and *Read_griddesc*) to
442 generate the CTM-ready chemically speciated, gridded hourly emissions in the NetCDF binary
443 format. The “**Plot Figures**” module is designed for generating various summary reports and
444 graphics to assist users in understanding the estimated automobile emissions inventory computed
445 by the CARS. The following section will describe the detailed processes of the “**Grid4AQM**”
446 module, which includes chemical, spatial, and temporal allocations.

447 The influence of temperature on emission processes are considered in the CARS model.
448 There are three temperature parameters in current CARS model such as “temp_max” for maximum
449 temperature, “temp_mean” for mean temperature, and “temp_min” for minimum temperature.
450 These temperature parameters will be applied to over the entire modeling domain during the
451 simulation period. Current CARS model version does not support to process gridded meteorology
452 data from the 3rd party meteorology models like Meteorology-Chemistry Interface Processor
453 (MCIP) from U.S. EPA., and Weather Research Forecasting (WRF) model from National Center
454 for Atmospheric Research (NCAR) yet. However, CARS can easily adopt various temporally
455 resolved temperature values by adjusting the CARS simulation period (i.e., day, week, month,
456 season, or annual).

457 **3.1 Chemical Speciation**

458 To support CTMs applications, the CARS needs to be able to convert inventory pollutants
459 into chemical lumped model species based on the choice of CTM chemical mechanisms. NO_x
460 includes nitric oxide (NO), nitrogen dioxide (NO₂), and nitrous acid (HONO). VOCs can represent
461 hundreds of different organic carbon species, such as benzene, acetaldehyde, and formaldehyde.
462 These grouped inventory pollutants cannot be directly imported into the chemical mechanism
463 modules in the CTM system and require chemical speciation allocation for CTMs to process them
464 during their chemical reactions. Therefore, the “**Grid4AQM**” module performs the chemical
465 species allocation step prior to the temporal and spatial allocations to generate the gridded hourly
466 emissions. The “*Read_chemical*” function in “**Grid4AQM**” module allows users to assign these
467 emission inventory pollutants to CTM-ready surrogate chemical species (a.k.a lumped chemical
468 species) by vehicle, engine, and fuel type. For example, VOC emissions from diesel busses can be
469 converted into the following composition based on its chemical allocation profile: alkanes (68%),
470 toluene (9%), xylenes (8%), alkenes (4%), ethylene (2%), benzene (1.3%), and unreactive
471 compounds (7%) when CB6 chemical mechanism is selected. Further details on the chemical
472 speciation profile input formats are available in the CARS user’s guide.

473 **3.2 Spatial Allocation**

474 The “**Calculate district emissions**” module calculates not only the total district emissions
475 but also road link-specific emissions based on road link-specific AADT data from road network
476 GIS shapefiles. The “**Calculate district emissions**” module first gets the district total vehicle
477 emissions (Eq. 2) based on the district-level VKTs, and then the normalized district total emissions
478 by district weight factor, ω_d (Eq. 13). Afterwards, the normalized district total emissions are
479 redistributed into every road link using road link-level weight factors ($\omega_{d,l}$) (Eq. 15). The district
480 total emissions from Eq. (2) and from Eq. (15) remain the same. Then the computed road link-

481 level emissions then will be converted into grid cell emissions using the modeling domain grid cell
482 fractions computed in the “*Read_griddesc*” function in the “**Grid4AQM**” module.

483 **3.3 Temporal Allocation**

484 Once chemical and spatial allocations are completed, the final step to support CTM
485 application is a temporal allocation that converts the annual total emissions from the “**Calculate**
486 **district emissions**” module into hourly emissions. The “*Read_temporal*” temporal allocation
487 function in the “**Grid4AQM**” module converts the annual emission rate ($t\ yr^{-1}$) to the hourly
488 emission rate ($mol\ hr^{-1}$) using monthly, weekly, and weekday/weekend diurnal temporal profiles.
489 This module processes these temporal profile inputs, which are the monthly (January - December),
490 weekly (Monday - Sunday), and weekday/weekend 24 hour profile tables (0:00-23:00 LST). The
491 users can assign these temporal profiles with a combination of vehicle, engine, fuel, and road types
492 to enhance their temporal representations in detail.

493 **3.4 Chemical Transport Model Emissions**

494 The main goal of the “**Grid4AQM**” module is to generate temporally, chemically, and
495 spatially enhanced CTM-ready gridded hourly emissions. First, it reads the CTM modeling domain
496 configuration and then overlays it over the road network GIS shapefile and district-boundary
497 shapefile to define the modeling domain. This overlaying process between the road network,
498 district boundary GIS shapefiles, and modeling domain allows the “**Grid4AQM**” module to
499 compute the fraction of road links that intersects with each grid cell. Figure 6 demonstrates how
500 the district boundary and road network GIS shapefiles are used to perform the spatial allocation
501 processes in CARS. Figure 6a is a native road link shapefile of Seoul with AADT, VKT, district
502 ID, and road type. Figure 6b presents an overlay of two districts’s road links (purple and blue) over
503 the selected region. State total emissions will be renormalized into weighed district total emission
504 data and then redistributed into the road link. Figure 6c illustrates how the weighted road link-
505 level emissions get allocated into modeling grid cells for CTMs. The link-level VKT ($VKT_{d,r,l}$)
506 from Eq. (12) will be used to compute a total of traffic activity fractions by grid cell and then use
507 that to assign the link-level emissions from Eq. (2) into each grid cell. When a road link intersects
508 with multiple grid cells, the “**Grid4AQM**” module will weigh the emissions by the length of the
509 link that intersects with each grid cell. It should be noted that current CARS model can only
510 generate the Community Multiscale Air Quality (CAMQ)-ready gridded hourly emissions in
511 format of IOAPI (Input/Output Applications Programming Interface) based on NetCDF format.

512 Through the overlay process, the CARS model can generate various types of output data,
513 such as total district emissions, link-level emissions, and CTM-ready gridded emissions. For
514 example, the CO vehicle emissions from the Seoul metropolitan in South Korea are presented in
515 three different output formats in Fig. 7. Figure 7a shows the annual mobile PM_{2.5} emissions by

516 district. The road link level annual emissions are presented in Fig. 7b. Furthermore, the CARS
517 applies the link-level emissions from Fig. 7b to generate the hourly grid cell emission data with a
518 1 km × 1 km resolution for the CTM in Fig. 7c.

519 **3.5 National Control Strategy Application**

520 One of the unique features in the CARS compared to other mobile emissions models is that
521 it can promptly develop controlled mobile emissions responding to the national emergency high
522 PM_{2.5} episodes. It is very common to experience high PM_{2.5} episodes, especially during the
523 wintertime in South Korea due to domestic and international primary and secondary air pollutants
524 emissions. When the 72 hour forecasted PM_{2.5} concentration exceeds the average 50 µg/m³ (0:00-
525 16:00 LST), the national PM_{2.5} emergency control strategy is activated for ten days. It applies a
526 nationwide vehicle restriction policy within 24 hours. It enforces a limit on what kind of vehicles
527 can be operated on a certain date. The restrictions can be applied in the following ways: the
528 closures of public parks and government facilities, and restrictions of certain vehicles based on
529 their fuel type and age, which is a major factor of engine deterioration. This policy will limit the
530 number of vehicles on the network roads significantly, which could reduce primary PM_{2.5} and
531 precursor pollutant (NO_x, NH₃, and VOC) emissions, especially from heavily populated
532 metropolitan regions (Choi et al., 2014; Kim et al., 2017a; Kim et al., 2017b; Kim et al., 2017c).

533 To understand the impacts of an even/odd vehicle restriction policy in real-time, we need to
534 quickly develop a rapid control response emissions for the air quality forecast modeling system.
535 The process of generating the controlled mobile emissions can take a long time if we start fresh.
536 Thus, we have implemented this control strategy as an optional “**Control Factors**” function in the
537 “**Calculate district emissions**” in the module for users to quickly and easily generate the
538 controlled mobile emissions with consideration of the limited number of vehicles based on the
539 vehicle, engine, fuel, and vehicle manufactured year. A one hundred percent (100%) control factor
540 means that there are no emissions from those selected vehicles.

541 Because of the modularization system in the CARS, we can bypass some computationally
542 expensive data processing modules (i.e., “**Process activity data**”, “**Process emission factors**”,
543 and “**Process shape file**”) and let the “**Calculate district emissions**” module quickly apply control
544 factors while it computes the district-level mobile emission inventory from Eq. (2). This will allow
545 users to reduce the computational time to generate the controlled mobile emissions under a specific
546 control scenario and develop the controlled CTM-ready gridded hourly emissions using the
547 “**Grid4AQM**” module.

548 **3.6 Computational Time**

549 While the CARS can generate a high-quality spatiotemporal emission inventory for
550 policymakers, stakeholders, and air quality modelers, it is quite critical for the CARS to generate

551 these complex mobile emissions effectively and accurately without being at the expense of
552 computational time. This is especially important to meet the needs for an air quality forecast
553 modeling system responding to a national emergency control strategy implementation.

554 In this section, we will discuss the details of the CARS computational modeling performance.
555 While the CARS model has been highly optimized, the modularization of CARS has also improved
556 its modeling performance with optional module runs. The breakdown of module-specific
557 computational time estimates based on the benchmark CARS runs are listed in Table 1. The
558 benchmark CARS case includes a total of 24,383,578 daily VKT datasets from KSTA over two
559 different years, 84,608 emission factors for all pollutants across a combination of vehicle-age-
560 engine-fuel types, 385,795 road links from the GIS road network shapefiles, 5,150 districts/16-
561 states boundary GIS shapefile, and 5,494 grid cells (=82 rows and 67 columns) for CTMs. Without
562 any computational parallelization, the total processing time of all six modules usually takes around
563 a half hour to generate a single day CTM-ready gridded hourly emission file. However, it can be
564 further shortened to 25-30 minutes on a higher performance computer. Because of the modular
565 system implemented in the CARS, generating one month (31 days) long gridded hourly emissions
566 from CTMs do not require over 15 computational hours, but only around 100 minutes on high-
567 performance computers. The maximum usage of RAM can reach up to 11 GB. Table 1 shows the
568 breakdown of computational time by each module from two different hardwares (desktop and
569 laptop computers). The numbers in parentheses beside the “Grid4AQM” module is the
570 computational time for a single day versus 31 days. While the “Grid4AQM” module takes an
571 average of 4.9 minutes for a single day emissions generation, processing a consecutive 31 days
572 saves 46% more time, decreasing from 151.9 minutes (=4.9 minutes * 31 days) to 81.6 minutes.

573 **4 Results**

574 **CARS and CAPSS Comparison**

575 The CARS model calculates the 2015 onroad automobile emissions based on the latest
576 2015 emission factors and the 2015-2017 vehicle activity database in South Korea. The annual
577 total emissions from CARS are compared against the ones from NIER CAPSS in Table 2. The
578 CARS model estimated the following annual total emissions in units of metric tons per year (t yr⁻¹):
579 NO_x (301,794); VOC (61,186); CO (373,864), NH₃ (12,453); PM_{2.5} (10,108), and SO_x (172.0).
580 Compared to NIER CAPSS, the CARS overestimated all pollutants except for NO_x (-18% decrease)
581 and SO_x (-17% decrease). It overestimated the emissions of VOC by 33%, PM_{2.5} by 15%, CO by
582 52%, and NH₃ by 24%. Both NIER CAPSS and CARS shared the same emission factor tables,
583 which hold over 84,608 emission factors for all pollutants across a combination of vehicle, age,
584 engine, and fuel types.

585 The difference between CAPSS and CARS approaches are caused by three reasons: First,
586 the number of vehicles used in CARS is slightly higher (6%) than CAPSS data (1.3 out of 23

587 million), as well as other key traffic-related activity inputs (i.e., vehicle age distribution, averaged
588 speed distribution, etc). Secondly, the vehicle speed information assigned by vehicle and road type
589 play a critical role in the differences between CAPSS and CARS. The CAPSS calculation was
590 based on the road-specific mean speed value or 80% of the speed limit as an input of vehicle
591 operating speed by three road types (rural, urban, and expressway). In other words, CAPSS only
592 assigns a “single-speed value” for each road type, and does not encounter the variation of vehicle
593 speed during its operation on roads into the emissions calculation. Most running exhaust emissions
594 occur during a vehicle’s low-speed operation due to its incomplete combustion of fuel, and it is
595 critical to accurately represent the emissions across various speed bins in order to compute the
596 correct emissions. The CARS model has an option to apply the average speed distribution (ASD)
597 over 16 speed bins for eight road types (Fig. 4). The CARS speed distribution process can better
598 represent the speed variations of vehicle speeds for each road type. A detailed analysis of the
599 impact of vehicle speed will be discussed later in this chapter. Lastly, other advanced processes in
600 the CARS, such as link-level AADT and district-level vehicle data (5,150 districts in South Korea),
601 can reflect more spatial detail and variation than the CAPSS. The CAPSS only considers state-
602 level data (17 states in South Korea) and five road types (interstate expressway, urban highway,
603 rural highway, urban local, and rural local).

604 Figure 8 illustrates more details about the difference between the annual emissions from
605 CARS to the CAPSS by pollutants and vehicle types. Sedan vehicles show the largest increase of
606 VOC (33%), CO (41%), and NH₃ (23%) in the CARS relative to CAPSS because almost 56% of
607 total vehicle count (13.5 million) is composed of sedan vehicles. Also, sedan vehicles contribute
608 51% of total VOC and 61% of total CO annual emissions. The VOC and CO emissions from sedans
609 are largely affected by the average speed distribution process when compared to other vehicle
610 types. Similarly, the largest decreases of NO_x (-16%) and SO_x (-18%) are from trucks because they
611 are significant NO_x (~50%) and SO_x contributors (~27%) and their emission factors are sensitive
612 to vehicle speed.

613 **Onroad Emissions Analysis**

614 The CARS is a bottom-up emissions model, which utilizes local individual vehicle activity
615 data, detailed local emission factors for every vehicle and fuel type, and localized inputs such as
616 average speed distribution by road type and deterioration factor. It allows users to assess the
617 detailed breakdown of localized emission contributions. Table 3 represents the individual air
618 pollutants (NO_x, VOC, PM_{2.5}, CO, NH₃, and SO_x) emission contributions (t yr⁻¹), fractions (%),
619 and impact factors (IF) by the vehicle type and fuel system. The IF is defined by the normalized
620 annual emissions with vehicle counts of each category (kg yr⁻¹ per vehicle). The CARS also can
621 provide the average daily VKT per vehicle, which is the total daily VKT divided by vehicle
622 numbers, to explain the emission contributions in Appendix D.

623 Diesel-fueled vehicles contribute the most of NO_x emissions, which is over 85.3% (257,305
624 t yr⁻¹), although the number of diesel vehicles only amounts to approximately 35% of the total
625 vehicles (Table 3a). While the diesel trucks emitted 49.1% (148,246 t yr⁻¹) of total NO_x with an IF
626 value of 47.9 (kg yr⁻¹), the highest impact (IF = 340 kg yr⁻¹) occurred from diesel buses with only
627 a 8.51% contribution to the total NO_x emissions. This is caused by the highest average daily VKT
628 from diesel buses compared to other vehicles, which is expected in a highly populated metropolitan
629 area like Seoul, South Korea. A diesel bus generally has a 3-5 times higher daily VKT (180 km d⁻¹
630 ¹) than other common vehicles (gasoline sedan: 34 km d⁻¹, diesel truck: 57 km d⁻¹). The second-
631 largest vehicle type is the CNG (compressed natural gas) bus (248 kg yr⁻¹), which also has a higher
632 VKT. Their average daily VKT is 212 km d⁻¹, with only a 3.1% NO_x contribution.

633 For VOC emissions, over 12 million gasoline vehicles cause 52.1% (31,885 t yr⁻¹) of the
634 total VOC emissions, and the gasoline sedan is the highest contributor across all vehicle types,
635 which is over 28,434 t yr⁻¹ (46.5%) (Table 3b). Unlike NO_x emissions, diesel vehicles only
636 contribute 23.0% (14,070 t yr⁻¹) of the total VOC emissions. Across the vehicle fuel types, the IF
637 outcome indicates that CNG vehicles have the highest IF values for VOC, which is 247 kg yr⁻¹ due
638 to the relatively high VOC contribution (19% over total VOC) and a low number of heavy CNG
639 vehicles. The IF of CNG trucks are 77.2 kg yr⁻¹, but only contribute 0.2% to total VOC emissions.
640 The IF of the CNG bus is 320 kg yr⁻¹ and emits 19.5% of the total VOC. Comparing the IFs of
641 buses across fuel types, the CNG bus emits less NO_x but higher VOC than a diesel vehicle. Each
642 CNG bus has about 33 times higher IF of VOC (320 kg yr⁻¹) than a diesel bus (9.51 kg yr⁻¹), and
643 CNG buses released slightly lower NO_x (248 kg yr⁻¹) than diesel buses (340 kg yr⁻¹) (Table 3a and
644 3b). It indicates that a CNG bus is better for rural areas and a diesel bus is better for urban areas to
645 control ozone, because the rural area is usually NO_x limited for ozone formation and urban areas
646 are VOC limited.

647 The current South Korea NIER currently does not have the PM emission factors from tire
648 and brake wear, which are the highest contributors of PM_{2.5} emissions from onroad vehicles (Hugo
649 A.C. et al., 2013; Fulvio Amato et al., 2014). Once the emission factors of tire and brake wear are
650 prepared, those emissions can be computed by CARS. For that reason, diesel vehicles become the
651 major source of PM_{2.5} emissions, which contributes over 98.5% (9,959 t yr⁻¹) of the PM_{2.5}
652 emissions based on the CARS 2015 emissions (Table 3c). The diesel truck, SUV, and van are the
653 three major sources, and their contributions of total PM_{2.5} are 53.6%, 21.4%, and 11.2%,
654 respectively. Although over 52% of the vehicles are gasoline vehicles, their primary PM_{2.5}
655 contribution is limited to 1.44%. The diesel bus has the highest IF (2.83 kg yr⁻¹), which is caused
656 by the largest average daily VKTs.

657 Similar to VOC emissions, CO is mostly emitted through the tailpipe due to incomplete
658 internal combustion of fuel and share similar emissions distributions across vehicle and fuel types
659 (Table 3d). Gasoline vehicles contribute most of the CO (220,390 t yr⁻¹, 59.0%), and sedan vehicles
660 are the primary source (178,121 t yr⁻¹, 47.6%) of this out of all gasoline vehicles. Across vehicle

661 types, bus shows the highest IF of CO (81.2 kg yr⁻¹) due to its largest daily VKT. CO is the most
662 abundant pollutant released from vehicles (373,864 t yr⁻¹) across all pollutants from onroad
663 automobile sources. Although CO is much less reactive than other vehicle VOCs (Rinke and
664 Zetzsch, 1984; Liu and Sander, 2015), the majority of CO emissions from onroad automobile
665 sources plays a critical role in generating 30% of hydroperoxyl radicals (HO₂) and causing ozone
666 formation in urban areas (Pfister et al., 2019). Thus, CO is also another crucial precursor to ozone
667 formation in urban areas.

668 SO_x emissions are related to the sulfur content within the fuel component; diesel has a
669 higher sulfur content than any other fuels. Most SO_x is contributed by diesel vehicles (93.8 t yr⁻¹,
670 54.5%) (Table 3e). Within diesel vehicles, trucks provide 26.5% of SO_x (45. t yr⁻¹). Although the
671 SO_x from sedan vehicles are slightly higher (~3.3%) than diesel trucks, the number of diesel trucks
672 is only 29.6% of the number of gasoline sedans. Thus, diesel trucks have a higher IF than gasoline
673 sedans. Across vehicle types, buses have the highest IF (0.095 kg yr⁻¹) of SO_x, and diesel buses in
674 particular have the largest IF at 0.143 kg yr⁻¹.

675 The NH₃ emissions table (table 3f) indicates that 98.7% of NH₃ is from gasoline vehicles
676 while diesel trucks only contribute 1.13%. The IF result also shows that the gasoline sedan has the
677 most significant impact per vehicle (1.17 kg yr⁻¹).

678 According to the vehicle activity and the CARS model results, nearly half of the total
679 vehicles (24.3 million) are gasoline sedans (10.4 million, 42.8%), and gasoline sedan vehicles
680 contributed most of the VOC and CO emissions (46.5% and 47.6%), but only 7.7% of the total
681 NO_x emissions. The number of diesel vehicles is 8.6 million (35.4%); however, they emitted about
682 85.3% of the total NO_x and 98.5% of the primary PM_{2.5}. These results indicated that the annual
683 traffic-related mobile emissions are not only affected by the number of vehicles, but also by
684 different vehicle and fuel types. Therefore, this study normalized the annual emissions by the
685 number of vehicles to confirm the emission composition by individual vehicle types.

686 **Average Speed Impact Study**

687 The CARS can also optionally apply the average speed distribution (ASD) by road type to
688 compute more realistic mobile emissions on the road network when compared to using a current
689 single average speed value for each road type (Appendix E). Applying the ASD will generate a
690 much better representation of actual traffic patterns from each road type. To understand the impacts
691 of ASD application, we performed sensitivity runs between using a single-speed to the ASD
692 application (Appendix F). The ASD data was described in Fig. 4, and the road-specific average
693 single-speed values were developed based on the weighted average method using the same ASD
694 data. Appendix E and S6 describes the details of ASD as well as road-specific speed values.

695 Figure 9a shows the differences in total emissions between two scenarios and is organized
696 by pollutant. The single-speed scenario largely underestimates the emissions across all pollutants
697 compared to the ones from the ASD scenario. NO_x (16%), VOC (40%), and CO (30%) were

698 especially underestimated. The difference is caused by the lack of low-speed bins ($<16 \text{ km h}^{-1}$)
699 representation when a single average speed approach was used. Higher emissions are emitted while
700 vehicles are operated with low-speed bins, which decreases the combustion efficiency of ICE and
701 releases more pollutants.

702 Figure 9b shows the road-specific breakdown between the ASD and single speed scenarios
703 to understand the impacts of vehicle operating speeds on onroad automobile emissions. In this
704 figure, each color indicates the emissions percentage differences by road types. Other than NH_3 ,
705 significant discrepancies happened between local urban roads (5.8%), highways (3.9%), and urban
706 highways (3.0%). Other pollutants, VOC, $\text{PM}_{2.5}$, CO, and SO_x , have similar fractions of road types.
707 This phenomenon is caused by low-speed conditions ($<16 \text{ km h}^{-1}$) and the fractions of road VKT
708 contributions (Appendix C). The lower speeds cause the incomplete combustion of ICE and
709 increase the emission rate. Also, local urban roads, highways, and urban highways have higher
710 road VKT contributions at 17%, 18%, and 12%, respectively (Appendix C) than rural roads.
711 Higher emissions from low speed conditions from these high contribution roads (urban local, urban
712 highway, and highway) caused these significant differences between the ASD and single-speed
713 approaches. Although the interstate expressway has the largest VKT contribution (41%), it also
714 has the lowest fraction of low-speed bins (2%). That is why the difference between the ASD and
715 single speed scenarios on interstate expressways is less than 1%. In general, NH_3 emission factors
716 do not change by vehicle operating speed, so the ASD impact is quite minimal.

717 **5 Conclusions**

718 The CARS is a bottom-up automobile emissions model that utilizes the localized traffic-
719 related activity and emission factors input datasets to generate high quality localized bottom-up
720 emissions inventories for policymakers, stakeholders, and research community as well as
721 temporally and spatially enhanced hourly gridded emissions for CTMs. First, the CARS model
722 employs the daily VKTs for all registered vehicles and the emission factors function to compute
723 district-level total daily emissions for each vehicle. To reflect realistic traffic patterns, the CARS
724 model computes and utilizes link-level VKTs ($=\text{link-length} \times \text{AADT}$) from the road network GIS
725 shapefiles to redistribute the original district-level total emissions into spatially enhanced road
726 link-level emissions. It can also optionally implement a control strategy as well as road restriction
727 rules to improve the quality of local emission inventories and meet the needs of users.

728 The CARS model is a fully modularized and computationally optimized python-based
729 bottom-up mobile emissions model that can effectively process a huge dataset to calculate high
730 quality spatiotemporal county-level, road link-level and grid cell-level mobile emissions. We
731 believe that the implementation of the ASD into the CARS improves the representation of onroad
732 automobile emissions from the road network when compared to a single-speed for each road type
733 approach. It allows the CARS to have a better representation of low speed ($<16 \text{ km h}^{-1}$) vehicle

734 emissions. We believe that CARS model's versatile spatiotemporal bottom-up automobile
735 emissions and the in-depth analysis feature can assist government policymakers and stakeholders
736 to develop the rapid responsive emission abatement strategies as a response to the South Korea's
737 national PM_{2.5} emergency control strategy that enforces the nationwide vehicle restriction policy
738 within 24 hours.

739 **Code Availability:**

740 The source code of the CARS model public release version 1.0 can be downloaded from the
741 Github release website:

742 <https://github.com/bokhaeng/CARS/releases/tag/CARSv1.0>

743

744

745 **Digital Object Identifier (DOI) for the CARS version 1.0:**

746 <https://zenodo.org/record/5033314#.YNzDrC1h001>

747

748

749 **Installation Package for CARS version 1.0:**

750 The CARS version 1.0 installation package comes with the complete inputs and outputs datasets
751 for users to confirm their proper installation on their computers and can be downloaded from the
752 Github release website:

753 https://github.com/bokhaeng/CARS/releases/download/CARSv1.0/CARS_v1.0_public_release_package_25June2021.zip

754

755

756

757 **User's Guide Documentation:**

758 The CARS version user's guide documentation can be accessed through the Github repository:

759 https://github.com/bokhaeng/CARS/tree/master/docs/User_Manual

760

761

762 **Data availability:**

763 All the datasets, excel and python scripts used in this manuscript for the data analysis are
764 uploaded through GMD website along with a supplemental appendix document.

765

766 **Author contribution**

767 Dr. B.H. Baek and Dr. Jung-Hun Woo are lead researchers in this study. Dr. Rizzieri Pedruzzi
768 develop the source code of CARS model, Dr. Minwoo Park tested the model and provided the
769 model input data. Dr. Chi-Tsan Wang analyzed the model result and prepared the manuscript.
770 Younha Kim, Chul-Han Song, analyzed the model result and provided comments.

771

772

773 **Competing interests**

774 The Authors declare that they have no conflict of interest.

775 **Acknowledgments**

776 This research was funded by the National Strategic Project-Fine Particle of the National Research
777 Foundation (NRF) of Korea funded by the Ministry of Science and ICT (MSIT), the Ministry of
778 Environment (ME), the Ministry of Health and Welfare (MOHW) (NRF-2017M3D8A1092022),
779 and by the Korea Environmental Industry & Technology Institute (KEITI) through the Public
780 Technology Program based on Environmental Policy Program, funded by Korea Ministry of
781 Environment (MOE) (2019000160007).

782

783 **References**

784 Safety flare for burning combustible gas - has tangential inlet for non-flammable gas between
785 housing and stack, in, Shell Oil Co (Shel-C).

786 Anaconda, Anaconda python: <https://www.anaconda.com/products/individual>, last access: May,
787 1st, 2020.

788 Appel, W., Chemel, C., Roselle, S., Francis, X., Hu, R.-M., Sokhi, R., Rao, S. T., and Galmarini,
789 S.: Examination of the Community Multiscale Air Quality (CMAQ) model performance over the
790 North American and European domains, *Atmospheric Environment*, 53, 142–155,
791 10.1016/j.atmosenv.2011.11.016, 2013.

792 Baek, B. H., and Seppanen, C., SMOKE v4.8.1 Public Release (January 29, 2021) (Version
793 SMOKEv481_Jan2021): <http://doi.org/10.5281/zenodo.4480334> last 2021.

794 Burnett, R., Chen, H., Szyszkowicz, M., Fann, N., Hubbell, B., Pope, C. A., Apte, J. S., Brauer,
795 M., Cohen, A., Weichenthal, S., Coggins, J., Di, Q., Brunekreef, B., Frostad, J., Lim, S. S., Kan,
796 H., Walker, K. D., Thurston, G. D., Hayes, R. B., Lim, C. C., Turner, M. C., Jerrett, M.,
797 Krewski, D., Gapstur, S. M., Diver, W. R., Ostro, B., Goldberg, D., Crouse, D. L., Martin, R. V.,
798 Peters, P., Pinault, L., Tjepkema, M., van Donkelaar, A., Villeneuve, P. J., Miller, A. B., Yin, P.,
799 Zhou, M., Wang, L., Janssen, N. A. H., Marra, M., Atkinson, R. W., Tsang, H., Quoc Thach, T.,
800 Cannon, J. B., Allen, R. T., Hart, J. E., Laden, F., Cesaroni, G., Forastiere, F., Weinmayr, G.,
801 Jaensch, A., Nagel, G., Concin, H., and Spadaro, J. V.: Global estimates of mortality associated
802 with long-term exposure to outdoor fine particulate matter, *Proceedings of the National*
803 *Academy of Sciences*, 115, 9592, 10.1073/pnas.1803222115, 2018.
804

805 Choi, D., Beardsley, M., Brzezinski, D., Koupal, J., and Warila, J.: MOVES Sensitivity
806 Analysis: The Impacts of Temperature and Humidity on Emissions
807 , available at: <https://www3.epa.gov/ttn/chief/conference/ei19/session6/choi.pdf> 2017.

808 Choi, K.-C., Lee, J.-J., Bae, C. H., Kim, C.-H., Kim, S., Chang, L.-S., Ban, S.-J., Lee, S.-J., Kim,
809 J., and Woo, J.-H.: Assessment of transboundary ozone contribution toward South Korea using
810 multiple source–receptor modeling techniques, *Atmospheric Environment*, 92, 118-129,
811 <https://doi.org/10.1016/j.atmosenv.2014.03.055>, 2014.

812 Cohen, A. J., Brauer, M., Burnett, R., Anderson, H. R., Frostad, J., Estep, K., Balakrishnan, K.,
813 Brunekreef, B., Dandona, L., Dandona, R., Feigin, V., Freedman, G., Hubbell, B., Jobling, A.,

- 814 Kan, H., Knibbs, L., Liu, Y., Martin, R., Morawska, L., Pope, C. A., III, Shin, H., Straif, K.,
815 Shaddick, G., Thomas, M., van Dingenen, R., van Donkelaar, A., Vos, T., Murray, C. J. L., and
816 Forouzanfar, M. H.: Estimates and 25-year trends of the global burden of disease attributable to
817 ambient air pollution: an analysis of data from the Global Burden of Diseases Study 2015, *The*
818 *Lancet*, 389, 1907-1918, 10.1016/S0140-6736(17)30505-6, 2017.
- 819
- 820 Dennis, R., Fox, T., Fuentes, M., Gilliland, A., Hanna, S., Hogrefe, C., Irwin, J., Rao, S. T.,
821 Scheffe, R., Schere, K., Steyn, D., and Venkatram, A.: A FRAMEWORK FOR EVALUATING
822 REGIONAL-SCALE NUMERICAL PHOTOCHEMICAL MODELING SYSTEMS, *Environ*
823 *Fluid Mech (Dordr)*, 10, 471-489, 10.1007/s10652-009-9163-2, 2010.
- 824 EEA: EMEP/EEO air pollutant emission inventory guidebook 2016, 2019.
- 825 Enthought, Enthought Canapy Python: <https://assets.enthought.com/downloads/edm/>, last
826 access: May, 1st, 2020.
- 827 Fallahshorshani, M., André, M., Bonhomme, C., and Seigneur, C.: Coupling Traffic, Pollutant
828 Emission, Air and Water Quality Models: Technical Review and Perspectives, *Procedia - Social*
829 *and Behavioral Sciences*, 48, 1794-1804, <https://doi.org/10.1016/j.sbspro.2012.06.1154>, 2012.
- 830 Fulvio Amato, Flemming R. Cassee, Hugo A.C. Denier van der Gon, Robert Gehrig, Mats
831 Gustafsson, Wolfgang Hafner, Roy M. Harrison, Magdalena Jozwicka, Frank J. Kelly,
832 TeresaMoreno, Andre S.H. Prevot, Martijn Schaap, Jordi Sunyer, Xavier Querol, Urban air
833 quality: The challenge of traffic non-exhaust emissions, *Journal of Hazardous Materials*, 275, 31-
834 36, <https://doi.org/10.1016/j.jhazmat.2014.04.053>, 2014.
- 835
- 836 Guevara, M., Tena, C., Porquet, M., Jorba, O., and Pérez García-Pando, C.: HERMESv3, a
837 stand-alone multi-scale atmospheric emission modelling framework – Part 1: global and regional
838 module, *Geosci. Model Dev.*, 12, 1885-1907, 10.5194/gmd-12-1885-2019, 2019.
- 839 Hogrefe, C., Rao, S. T., Kasibhatla, P., Hao, W., Sistla, G., Mathur, R., and McHenry, J.:
840 Evaluating the performance of regional-scale photochemical modeling systems: Part II—ozone
841 predictions, *Atmospheric Environment*, 35, 4175-4188, [https://doi.org/10.1016/S1352-](https://doi.org/10.1016/S1352-2310(01)00183-2)
842 [2310\(01\)00183-2](https://doi.org/10.1016/S1352-2310(01)00183-2), 2001a.
- 843 Hogrefe, C., Rao, S. T., Kasibhatla, P., Kallos, G., Tremback, C. J., Hao, W., Olerud, D., Xiu,
844 A., McHenry, J., and Alapaty, K.: Evaluating the performance of regional-scale photochemical

- 845 modeling systems: Part I—meteorological predictions, *Atmospheric Environment*, 35, 4159-
846 4174, [https://doi.org/10.1016/S1352-2310\(01\)00182-0](https://doi.org/10.1016/S1352-2310(01)00182-0), 2001b.
- 847 Hugo A.C. Denier van der Gon, Miriam E. Gerlofs-Nijland, Robert Gehrig, Mats Gustafsson,
848 Nicole Janssen, Roy M. Harrison, Jan Hulskotte, Christer Johansson, Magdalena Jozwicka,
849 Menno Keuken, Klaas Krijgsheld, Leonidas Ntziachristos, Michael Riediker & Flemming R.
850 Cassee: The Policy Relevance of Wear Emissions from Road Transport, Now and in the
851 Future—An International Workshop Report and Consensus Statement, *Journal of the Air &*
852 *Waste Management Association*, 63:2, 136-149, DOI: 10.1080/10962247.2012.741055, 2013
853
- 854 Ibarra-Espinosa, S., Ynoue, R., amp, apos, Sullivan, S., Pebesma, E., Andrade, M. d. F., and
855 Osses, M.: VEIN v0.2.2: an R package for bottom–up vehicular emissions inventories, *Geosci.*
856 *Model Dev.*, 11, 2209-2229, 10.5194/gmd-11-2209-2018, 2018a.
- 857 Ibarra-Espinosa, S., Ynoue, R., O'Sullivan, S., Pebesma, E., Andrade, M. D. F., and Osses, M.:
858 VEIN v0.2.2: an R package for bottom–up vehicular emissions inventories, *Geosci. Model Dev.*,
859 11, 2209-2229, 10.5194/gmd-11-2209-2018, 2018b.
- 860 IEMA, Inventário de Emissões Atmosféricas do Transporte Rodoviário de Passageiros no
861 Município de São Paulo.: <http://emissoes.energiaambiente.org.br>, last access: May,1st, 2017.
- 862 Jang, Y. K., Cho, K. L., Kim, K., Kim, H. J., and Kim, J.: Development of methodology for
863 estimation of air pollutants emissions and future emissions from on-road mobile sources.,
864 National Institute of Environmental Research, Incheon, Korea., available at: 2007.
- 865 Kaewunruen, S., Sussman, J. M., and Matsumoto, A.: Grand Challenges in Transportation and
866 Transit Systems, *Frontiers in Built Environment*, 2, 10.3389/fbuil.2016.00004, 2016.
- 867 Kim, B.-U., Bae, C., Kim, H. C., Kim, E., and Kim, S.: Spatially and chemically resolved source
868 apportionment analysis: Case study of high particulate matter event, *Atmospheric Environment*,
869 162, 55-70, <https://doi.org/10.1016/j.atmosenv.2017.05.006>, 2017a.
- 870 Kim, H. C., Kim, E., Bae, C., Cho, J. H., Kim, B. U., and Kim, S.: Regional contributions to
871 particulate matter concentration in the Seoul metropolitan area, South Korea: seasonal variation
872 and sensitivity to meteorology and emissions inventory, *Atmos. Chem. Phys.*, 17, 10315-10332,
873 10.5194/acp-17-10315-2017, 2017b.

- 874 Kim, H. C., Kim, S., Kim, B.-U., Jin, C.-S., Hong, S., Park, R., Son, S.-W., Bae, C., Bae, M.,
875 Song, C.-K., and Stein, A.: Recent increase of surface particulate matter concentrations in the
876 Seoul Metropolitan Area, Korea, *Scientific Reports*, 7, 4710, 10.1038/s41598-017-05092-8,
877 2017c.
- 878 L., W. P., and Heo, G.: Development of revised SAPRC aromatics mechanism, available at:
879 <https://www.engr.ucr.edu/~carter/SAPRC/saprc11.pdf> 2012.
- 880 Lee, D., Lee, Y.-M., Jang, K.-W., Yoo, C., Kang, K.-H., Lee, J.-H., Jung, S.-W., Park, J.-M.,
881 Lee, S.-B., Han, J.-S., Hong, J.-H., and Lee, S.-J.: Korean National Emissions Inventory System
882 and 2007 Air Pollutant Emissions, *Asian Journal of Atmospheric Environment*, 5-4, 278-291,
883 2011a.
- 884 Lee, D.-G., Lee, Y.-M., Jang, K.-W., Yoo, C., Kang, K.-H., Lee, J.-H., Jung, S.-W., Park, J.-M.,
885 Lee, S.-B., Han, J.-S., Hong, J.-H., and Lee, S.-J.: Korean National Emissions Inventory System
886 and 2007 Air Pollutant Emissions, *Asian Journal of Atmospheric Environment*, 5,
887 10.5572/ajae.2011.5.4.278, 2011b.
- 888 Lejri, D., Can, A., Schiper, N., and Leclercq, L.: Accounting for traffic speed dynamics when
889 calculating COPERT and PHEM pollutant emissions at the urban scale, *Transportation Research*
890 *Part D: Transport and Environment*, 63, 588-603, <https://doi.org/10.1016/j.trd.2018.06.023>,
891 2018.
- 892 Li, F., Zhuang, J., Cheng, X., Li, M., Wang, J., and Yan, Z.: Investigation and Prediction of
893 Heavy-Duty Diesel Passenger Bus Emissions in Hainan Using a COPERT Model, *Atmosphere*,
894 10, 106, 10.3390/atmos10030106, 2019.
- 895 Li, Q., Qiao, F., and yu, L.: Vehicle Emission Implications of Drivers Smart Advisory System
896 for Traffic Operations in Work Zones, *Journal of the Air & Waste Management Association*, 11,
897 10.1080/10962247.2016.1140095, 2016.
- 898 Liu, H., Guensler, R., Lu, H., Xu, Y., Xu, X., and Rodgers, M.: MOVES-Matrix for High-
899 Performance On-Road Energy and Running Emission Rate Modeling Applications, *Journal of*
900 *the Air & Waste Management Association*, 69, 10.1080/10962247.2019.1640806, 2019.
- 901 Liu, Y., and Sander, S. P.: Rate Constant for the OH + CO Reaction at Low Temperatures, *The*
902 *Journal of Physical Chemistry A*, 119, 10060-10066, 10.1021/acs.jpca.5b07220, 2015.

- 903 Luo, H., Astitha, M., Hogrefe, C., Mathur, R., and Rao, S. T.: A new method for assessing the
904 efficacy of emission control strategies, *Atmospheric Environment*, 199, 233-243,
905 <https://doi.org/10.1016/j.atmosenv.2018.11.010>, 2019.
- 906 Lv, W., Hu, Y., Li, E., Liu, H., Pan, H., Ji, S., Hayat, T., Alsaedi, A., and Ahmad, B.: Evaluation
907 of vehicle emission in Yunnan province from 2003 to 2015, *J. Clean Prod.*, 207, 814-825,
908 <https://doi.org/10.1016/j.jclepro.2018.09.227>, 2019.
- 909 Moussiopoulos, N., Vlachokostas, C., Tsilingiridis, G., Douros, I., Hourdakakis, E., Naneris, C.,
910 and Sidiropoulos, C.: Air quality status in Greater Thessaloniki Area and the emission reductions
911 needed for attaining the EU air quality legislation, *Sci. Total Environ.*, 407, 1268-1285,
912 <https://doi.org/10.1016/j.scitotenv.2008.10.034>, 2009.
- 913 Nagpure, A. S., Gurjar, B. R., Kumar, V., and Kumar, P.: Estimation of exhaust and non-exhaust
914 gaseous, particulate matter and air toxics emissions from on-road vehicles in Delhi, *Atmospheric
915 Environment*, 127, 118-124, [10.1016/j.atmosenv.2015.12.026](https://doi.org/10.1016/j.atmosenv.2015.12.026), 2016.
- 916 NIER: Study on Air Pollutant Emission Estimation Method in Transportation section(II) 11-
917 1480523-003573-01, National Archives of Korea, available at:
918 [https://www.archives.go.kr/next/manager/publishmentSubscriptionDetail.do?prt_seq=114054&p
age=1554&prt_arc_title=&prt_pub_kikwan=&prt_no](https://www.archives.go.kr/next/manager/publishmentSubscriptionDetail.do?prt_seq=114054&p
919 age=1554&prt_arc_title=&prt_pub_kikwan=&prt_no) 2018.
- 920 Ntziachristos, L., and Samaras, Z.: Speed-dependent representative emission factors for catalyst
921 passenger cars and influencing parameters, *Atmospheric Environment*, 34, 4611-4619,
922 [https://doi.org/10.1016/S1352-2310\(00\)00180-1](https://doi.org/10.1016/S1352-2310(00)00180-1), 2000.
- 923 Ntziachristos, L., Gkatzoflias, D., Kouridis, C., and Samaras, Z.: COPERT: A European road
924 transport emission inventory model, 491-504 pp., 2009.
- 925 Pedruzzi, R., Baek, B. H., and Wang, C.-T., CARS: <https://github.com/CMASCenter/CARS>,
926 last access: MAy, 1st, 2020.
- 927 Perugu, H., Ramirez, L., and DaMassa, J.: Incorporating temperature effects in California's on-
928 road emission gridding process for air quality model inputs, *Environ Pollut*, 239, 1-12,
929 [10.1016/j.envpol.2018.03.094](https://doi.org/10.1016/j.envpol.2018.03.094), 2018.

- 930 Perugu, H.: Emission modelling of light-duty vehicles in India using the revamped VSP-based
931 MOVES model: The case study of Hyderabad, *Transportation Research Part D: Transport and*
932 *Environment*, 68, 150-163, <https://doi.org/10.1016/j.trd.2018.01.031>, 2019.
- 933 Pfister, G., Wang, C.-t., Barth, M., Flocke, F., Vizuete, W., and Walters, S.: Chemical
934 Characteristics and Ozone Production in the Northern Colorado Front Range, *JGR*, 2019.
- 935 Pinto, J. A., Kumar, P., Alonso, M. F., Andreão, W. L., Pedruzzi, R., dos Santos, F. S., Moreira,
936 D. M., and Albuquerque, T. T. d. A.: Traffic data in air quality modeling: A review of key
937 variables, improvements in results, open problems and challenges in current research,
938 *Atmospheric Pollution Research*, 11, 454-468, <https://doi.org/10.1016/j.apr.2019.11.018>, 2020.
- 939 Rao, S. T., Galmarini, S., and Puckett, K.: Air Quality Model Evaluation International Initiative
940 (AQMEII): Advancing the State of the Science in Regional Photochemical Modeling and Its
941 Applications, *Bulletin of the American Meteorological Society*, 92, 23-30,
942 10.1175/2010BAMS3069.1, 2011.
- 943 Rodriguez-Rey et al. (2021): Rodriguez-Rey, D., Guevara, M., Linares, MP., Casanovas, J.,
944 Salmerón, J., Soret, A., Jorba, O., Tena, C., Pérez García-Pando, C.: A coupled macroscopic
945 traffic and pollutant emission modelling system for Barcelona, *Transportation Research Part D*,
946 92, <https://doi.org/10.1016/j.trd.2021.102725>, 2021.
- 947 Rinke, M., and Zetzsch, C.: Rate Constants for the Reactions of OH Radicals with Aromatics:
948 Benzene, Phenol, Aniline, and 1,2,4-Trichlorobenzene, *Berichte der Bunsengesellschaft für*
949 *physikalische Chemie*, 88, 55-62, 10.1002/bbpc.19840880114, 1984.
- 950 Russell, A., and Dennis, R.: NARSTO critical review of photochemical models and modeling,
951 *Atmospheric Environment*, 34, 2283-2324, [https://doi.org/10.1016/S1352-2310\(99\)00468-9](https://doi.org/10.1016/S1352-2310(99)00468-9),
952 2000.
- 953 Ryu, J. H., Han, J. S., Lim, C. S., Eom, M. D., Hwang, J. W., Yu, S. H., Lee, T. W., Yu, Y. S.,
954 and Kim, G. H.: The Study on the Estimation of Air Pollutants from Auto- mobiles (I) -
955 Emission Factor of Air Pollutants from Middle and Full sized Buses., in, *Transportation*
956 *Pollution Research Center, National Institute of Environmental Research, Incheon, Korea.*, 2003.
- 957 Ryu, J. H., Lim, C. S., Yu, Y. S., Han, J. S., Kim, S. M., Hwang, J. W., Eom, M. D., Kim, G. Y.,
958 Jeon, M. S., Kim, Y. H., Lee, J. T., and Lim, Y. S.: The Study on the Esti- mation of Air
959 Pollutants from Automobiles (II) - Emis- sion Factor of Air Pollutants from Diesel Truck., in,

960 Trans- portation Pollution Research Center, National Institute of Environmental Research,
961 Incheon, Korea., 2004.

962 Ryu, J. H., Yu, Y. S., Lim, C. S., Kim, S. M., Kim, J. C., Gwon, S. I., Jeong, S. W., and Kim, D.
963 W.: The Study on the Estimation of Air Pollutants from Automobiles (III) - Emission Factor of
964 Air Pollutants from Small sized Light-duty Vehicles., in, Transportation Pollution Research
965 Center, National Institute of Environmental Research, Korea., 2005.

966 Sallis, P., Bull, F., Burdett, P., Frank, P., Griffiths, P., Giles-Corti, P., and Stevenson, M.: Use of
967 science to guide city planning policy and practice: How to achieve healthy and sustainable future
968 cities, *The Lancet*, 388, 10.1016/S0140-6736(16)30068-X, 2016.

969 Smit, R., Kingston, P., Neale, D. W., Brown, M. K., Verran, B., and Nolan, T.: Monitoring on-
970 road air quality and measuring vehicle emissions with remote sensing in an urban area,
971 *Atmospheric Environment*, 218, 116978, <https://doi.org/10.1016/j.atmosenv.2019.116978>, 2019.

972 Sun, W., Duan, N., Yao, R., Huang, J., and Hu, F.: Intelligent in-vehicle air quality
973 management : a smart mobility application dealing with air pollution in the traffic, 2016.

974 Tominaga, Y., and Stathopoulos, T.: Ten questions concerning modeling of near-field pollutant
975 dispersion in the built environment, *Build. Environ.*, 105, 390-402,
976 <https://doi.org/10.1016/j.buildenv.2016.06.027>, 2016.

977 USEPA: Population and Activity of Onroad Vehicles in MOVES3, in, edited by: USEPA, 2020.

978 WHO, Ambient air pollution- a major threat to health and climate:
979 <https://www.who.int/airpollution/ambient/en/>, last 2019.

980 Xu, X., Liu, H., Anderson, J. M., Xu, Y., Hunter, M. P., Rodgers, M. O., and Guensler, R. L.:
981 Estimating Project-Level Vehicle Emissions with Vissim and MOVES-Matrix, *Transportation*
982 *Research Record*, 2570, 107-117, 10.3141/2570-12, 2016.

983 Yarwood, G., and Jung, J.: UPDATES TO THE CARBON BOND MECHANISM FOR
984 VERSION 6 (CB6), 2010.
985

986 **Tables**

987 **Table 1.** Computational processing time by CARS module based on the modeling setup: Total
 988 number of activity data = 24,383,578; Emission Factors = 84,608; GIS road links=385,795;
 989 districts/states=5,150/16; 9km×9km grid cells=5,494 (82 columns× 67 columns).

No	Module	Desktop i7 (minutes)	Laptop i9 (minutes)	Averaged Time (minutes)
1	Process activity data	1.8	1.5	1.7
2	process emission factors	1.1	0.8	1.0
3	Process shape file	9.9	7.3	8.6
4	Calculate district emissions	6.4	5.7	6.1
5	Grid4AQM [31days]	4.8 [75.9]	5.0 [87.2]	4.9 [81.6]
6	Plot figures	6.2	5.4	5.8
Total [31days]		30.2 [101.3]	25.7 [107.9]	28.1[104.8]

990

991

992

993 **Table 2.** The total emissions comparison between CARS and CAPSS for the 2015 emission.

Emission Inventory	Pollutants (t yr ⁻¹)					
	NO _x	VOC	PM2.5	CO	SO _x	NH ₃
CARS 2015	301,794	61,186	10,108	373,864	172	12,453
CAPSS 2015	369,585	46,145	8,817	245,516	209	10,079

994

995

996 **Table 3.** The summary tables of emissions (t yr⁻¹), contributions (%), and impact factor (IF, kg yr⁻¹) per vehicle for criteria air pollutants (CAPs) by vehicle and fuel types: (a) for NO_x; (b) VOC;
 997
 998 (c) for PM_{2.5}; (d) for CO; (e) for SO_x; and (f) for NH₃.
 999

1000 (a) NO_x

Vehicle	Gasoline		Diesel		LPG		CNG		Hybrid		Total	
	Emission	IF	Emission	IF	Emission	IF	Emission	IF	Emission	IF	Emission	IF
Sedan	20,219 (6.70%)	1.94	14,783 (4.90%)	12.8	8,159 (2.77%)	4.49	12 (0.00%)	1.26	65 (0.02%)	0.39	43,239 (14.3%)	3.19
Truck	23 (0.01%)	5.54	148,246 (49.1%)	47.9	920 (0.31%)	4.55	88 (0.03%)	66.4	-	-	149,277 (49.5%)	45.2
Bus	0 (0.00%)	0.97	25,677 (8.51%)	340	-	-	9,260 (3.07%)	248	0 (0.00%)	1.77	34,938 (11.6%)	333
SUV	159 (0.05%)	1.19	39,565 (13.1%)	11.4	175 (0.06%)	8.54	0 (0.00%)	1.60	1 (0.00%)	0.42	39,900 (13.2%)	11.0
Van	14 (0.00%)	4.78	16,659 (5.52%)	22.6	1,337 (0.44%)	6.80	0 (0.00%)	1.25	0 (0.00)	0.37	18,012 (6.00%)	19.2
Taxi	-	-	-	-	1,217 (0.40%)	2.11	-	-	-	-	1,217 (0.40%)	2.11
Special	1 (0.00%)	20.1	12,347 (4.10%)	152	0 (0.00%)	0.52	-	-	-	-	12,375 (4.10%)	151
Motorcycle	2,836 (0.94%)	1.31	-	-	-	-	-	-	-	-	2,836 (0.94%)	1.32
Total	23,253 (7.70%)	1.83	257,305 (85.3%)	29.9	11,809 (3.91%)	4.20	9,361 (3.10%)	36.7	66 (0.02%)	0.39	301,794 (100%)	13.3

1001
 1002 (b) VOC

Vehicle	Gasoline		Diesel		LPG		CNG		Hybrid		Total	
	Emission	IF	Emission	IF	Emission	IF	Emission	IF	Emission	IF	Emission	IF
Sedan	28,434 (46.5%)	2.73	629 (1.03%)	0.55	2,107 (3.44%)	1.16	3 (0.01%)	0.33	77 (0.13%)	0.47	31,250 (51.1%)	2.30
Truck	23 (0.04%)	5.44	8,194 (13.4%)	2.65	286 (0.47%)	1.41	102 (0.17%)	77.2	-	-	8,605 (14.1%)	2.61
Bus	0 (0.00%)	1.65	717 (1.17%)	9.51	-	-	11,942 (19.5%)	320	0 (0.00%)	0	12,659 (20.7%)	112
SUV	246 (0.40%)	1.84	2,441 (3.99%)	0.71	46 (0.08%)	2.25	0 (0.00%)	0.75	1 (0.00%)	0.55	2,733 (4.47%)	0.76
Van	21 (0.03%)	7.04	1,185 (1.94%)	1.61	393 (0.64%)	2.00	0 (0.00%)	0.45	0 (0.00%)	0	1,599 (2.61%)	1.71
Taxi	-	-	-	-	273 (0.45%)	0.47	-	-	-	-	273 (0.45%)	0.47
Special	1 (0.00%)	25.8	904 (1.48%)	11.1	0 (0.00%)	0.23	-	-	-	-	905 (1.48%)	11.0
Motorcycle	3,160 (5.16%)	1.46	-	-	-	-	-	-	-	-	3,160 (5.16%)	1.46
Total	31,885 (52.1%)	2.50	14,070 (23.0%)	1.64	3,106 (5.08%)	1.10	12,047 (19.7%)	247	78 (0.13%)	0.47	61,186 (100%)	2.51

1003
 1004 (c) PM_{2.5}

Vehicle	Gasoline		Diesel		LPG		CNG		Hybrid		Total	
	Emission	IF	Emission	IF	Emission	IF	Emission	IF	Emission	IF	Emission	IF
Sedan	144 (1.42%)	0.01	809 (8.00%)	0.70	0	0	0	0	3 (0.03%)	0.02	956 (9.46%)	0.07
Truck	0 (0.01%)	0	5,415 (53.6%)	1.75	0	0	0	0	-	-	5,415 (53.6%)	1.64
Bus	0	0	214 (2.11%)	2.83	-	-	0	0	0 (0.01%)	0.09	214 (2.11%)	1.89
SUV	2 (0.02%)	0.02	2,165 (21.4%)	0.63	0	0	0	0	0	0.02	2,167 (21.4%)	0.60
Van	0	0	1,127 (11.2%)	1.53	0	0	0	0	0	0.02	1,127 (11.2%)	1.20
Taxi	-	-	-	-	0	0	-	-	-	-	0	0
Special	0	0	230 (2.28%)	2.82	0	0	-	-	-	-	230 (2.28%)	2.81
Motorcycle	0	0	-	-	-	-	-	-	-	-	0	0
Total	146 (1.44%)	0.01	9,959 (98.5%)	1.16	0	0	0	0	3 (0.03%)	0.02	10,108 (100%)	0.41

1005
 1006

1007

1008

(d) CO

Vehicle	Gasoline		Diesel		LPG		CNG		Hybrid		Total	
	Emission	IF	Emission	IF	Emission	IF	Emission	IF	Emission	IF	Emission	IF
Sedan	178,121 (47.6%)	17.1	3,436 (0.92%)	2.98	42,886 (11.5%)	23.6	29 (0.01%)	2.91	177 (0.05%)	1.07	224,649 (60.1%)	16.6
Truck	254 (0.07%)	61.1	47,065 (12.6%)	15.2	9,088 (2.43%)	44.9	68 (0.02%)	51.4	-	-	56,475 (15.1%)	17.1
Bus	0 (0.00%)	19.3	7,633 (2.05%)	101	-	-	1542 (0.41%)	41.3	1 (0.00%)	4.64	9,176 (2.45%)	81.2
SUV	2,616 (0.70%)	19.6	13,401 (3.58%)	3.87	791 (0.21%)	38.6	0 (0.00%)	4.09	2 (0.00%)	1.15	16,808 (4.50%)	4.65
Van	131 (0.04%)	43.4	6,611 (1.77%)	8.97	8,032 (2.15%)	40.9	2 (0.00%)	6.53	0 (0.00%)	1.00	14,777 (3.95%)	15.8
Taxi	-	-	-	-	8,481 (2.27%)	14.7	-	-	-	-	8,481 (2.27%)	14.7
Special	13 (0.00%)	269	4,224 (1.13%)	51.7	1 (0.00%)	3.69	-	-	-	-	4,239 (1.13%)	51.7
Motorcycle	39,256 (10.5%)	18.2	-	-	-	-	-	-	-	-	39,256 (10.5%)	18.2
Total	220,390 (59.0%)	17.3	82,372 (22.0%)	9.57	69,281 (18.5%)	24.6	1641 (0.44%)	33.6	180 (0.05%)	1.07	373,864 (100%)	15.4

1009

1010

(e) SO_x

Vehicle	Gasoline		Diesel		LPG		CNG		Hybrid		Total	
	Emission	IF	Emission	IF	Emission	IF	Emission	IF	Emission	IF	Emission	IF
Sedan	51.3 (29.8%)	0.005	6.5 (3.79%)	0.006	8.28 (4.81%)	0.005	0	0	1.14 (0.67%)	0.007	67.2 (39.1%)	0.005
Truck	0.03 (0.02%)	0.008	45.5 (26.5%)	0.015	0.97 (0.57%)	0.005	0	0	-	-	46.5 (27.1%)	0.014
Bus	0 (0.00%)	0.003	10.8 (6.26%)	0.143	-	-	0	0	0.01 (0.01%)	0.047	10.8 (6.26%)	0.095
SUV	0 (0.00%)	0.000	18.2 (10.6%)	0.005	0.00 (0.00%)	0.000	0	0	0.01 (0.01%)	0.007	18.2 (10.6%)	0.005
Van	0.02 (0.01%)	0.006	5.5 (3.20%)	0.007	0.77 (0.45%)	0.004	0	0	0 (0.00%)	0.010	6.30 (3.66%)	0.007
Taxi	-	-	-	-	7.71 (4.49%)	0.013	-	-	-	-	7.71 (4.48%)	0.013
Special	0 (0.00%)	0.003	7.3 (4.27%)	0.090	0.00 (0.00%)	0.005	-	-	-	-	7.34 (4.27%)	0.090
Motorcycle	7.94 (4.62%)	0.004	-	-	-	-	-	-	-	-	7.94 (4.62%)	0.004
Total	59.3 (34.5%)	0.006	93.8 (54.5%)	0.011	17.7 (10.3%)	0.006	0	0	1.17 (0.68%)	0.007	172 (100%)	0.007

1011

1012

1013

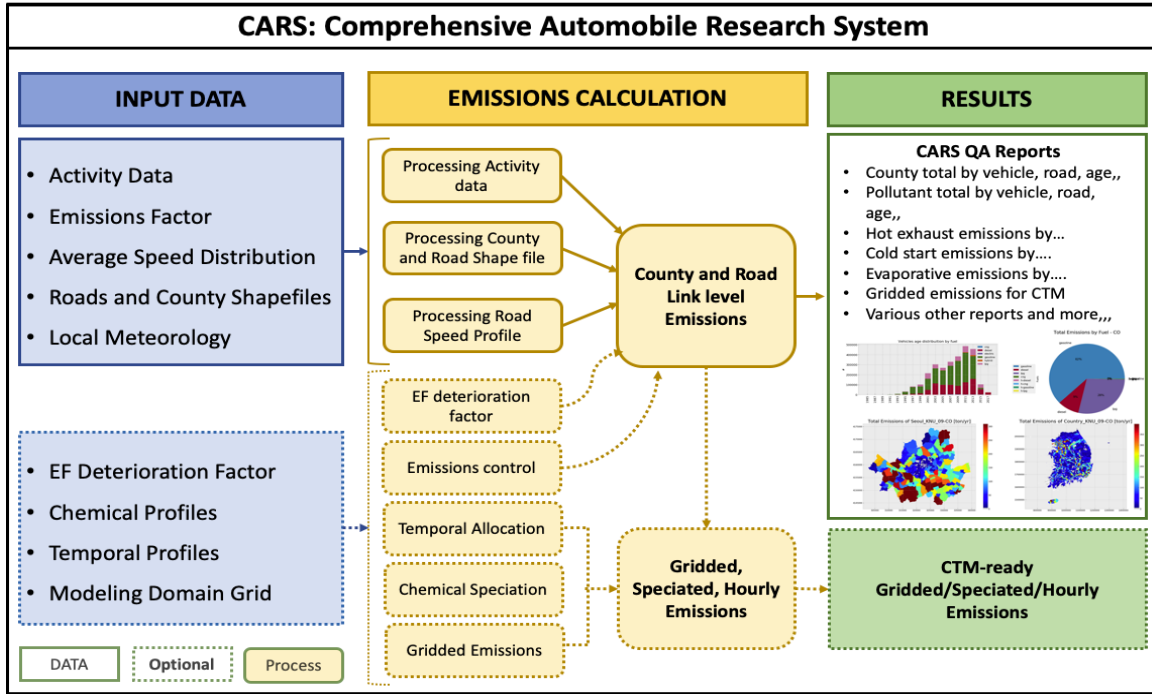
(e) NH₃

Vehicle	Gasoline		Diesel		LPG		CNG		Hybrid		Total	
	Emission	IF	Emission	IF	Emission	IF	Emission	IF	Emission	IF	Emission	IF
Sedan	12,225 (98.3%)	1.17	20 (0.16%)	0.02	0	0.00	0	0	19 (0.15%)	0.11	12,284 (98.6%)	0.91
Truck	0 (0.00%)	0.03	82 (0.66%)	0.03	0	0.00	0	0	-	-	82 (0.66%)	0.02
Bus	0 (0.00%)	0.09	15 (0.12%)	0.19	-	-	0	0	0 (0.00%)	0.51	15 (0.12%)	0.13
SUV	0 (0.00%)	0.00	0 (0.00%)	0.00	0	0.00	0	0	0 (0.00%)	0.16	0 (0.00%)	0.00
Van	0 (0.00%)	0.02	14 (0.11%)	0.02	0	0.00	0	0	0 (0.00%)	0.09	14 (0.11%)	0.01
Taxi	-	-	-	-	0	0.00	-	-	-	-	0 (0.00%)	0.00
Special	0 (0.00%)	0.01	10 (0.08%)	0.12	0	0.00	-	-	-	-	10 (0.08%)	0.12
Motorcycle	49 (0.39%)	0.02	-	-	-	-	-	-	-	-	49 (0.39%)	0.02
Total	12,293 (98.7%)	0.97	141 (1.13%)	0.02	0	0.00	0	0	19 (0.16%)	0.12	12,453 (100%)	0.51

1014

1015

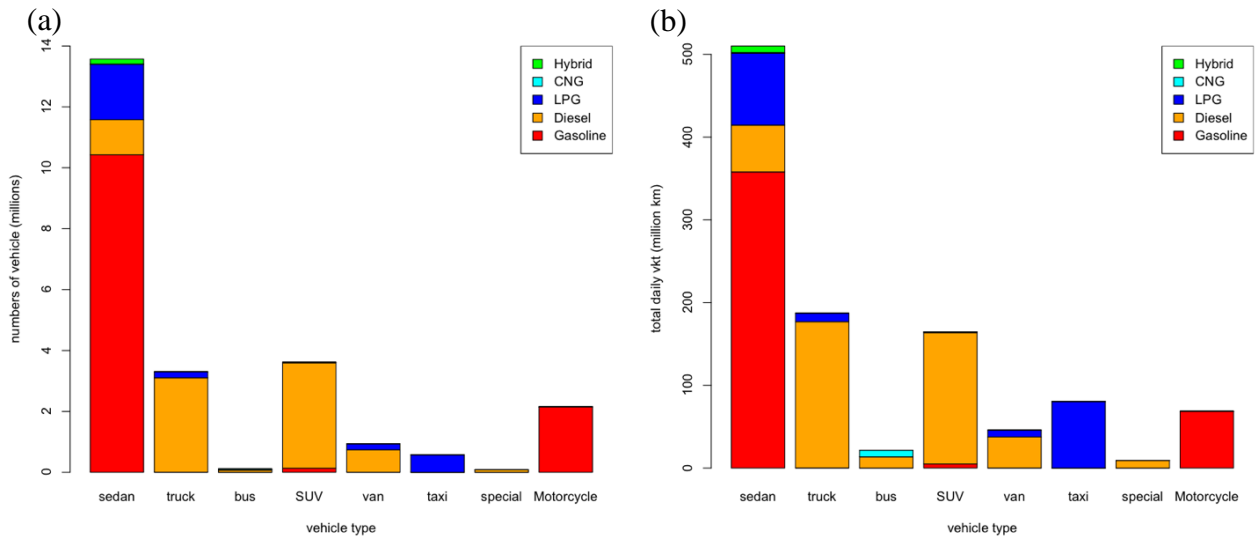
1016 **Figures**



1017

1018 **Figure 1.** CARS schematic methodology to estimate mobile emissions.

1019

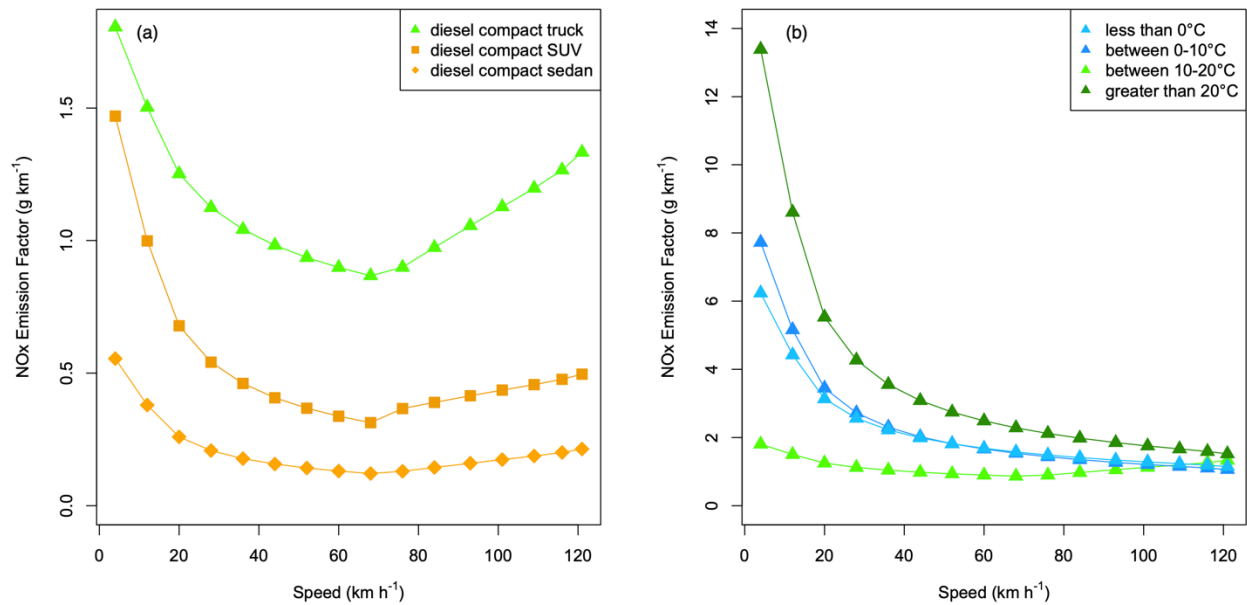


1020

1021 **Figure 2.** (a) The number of vehicles by vehicle and fuel types and (b) the total daily VKT by
 1022 vehicle and fuel types in South Korea.

1023

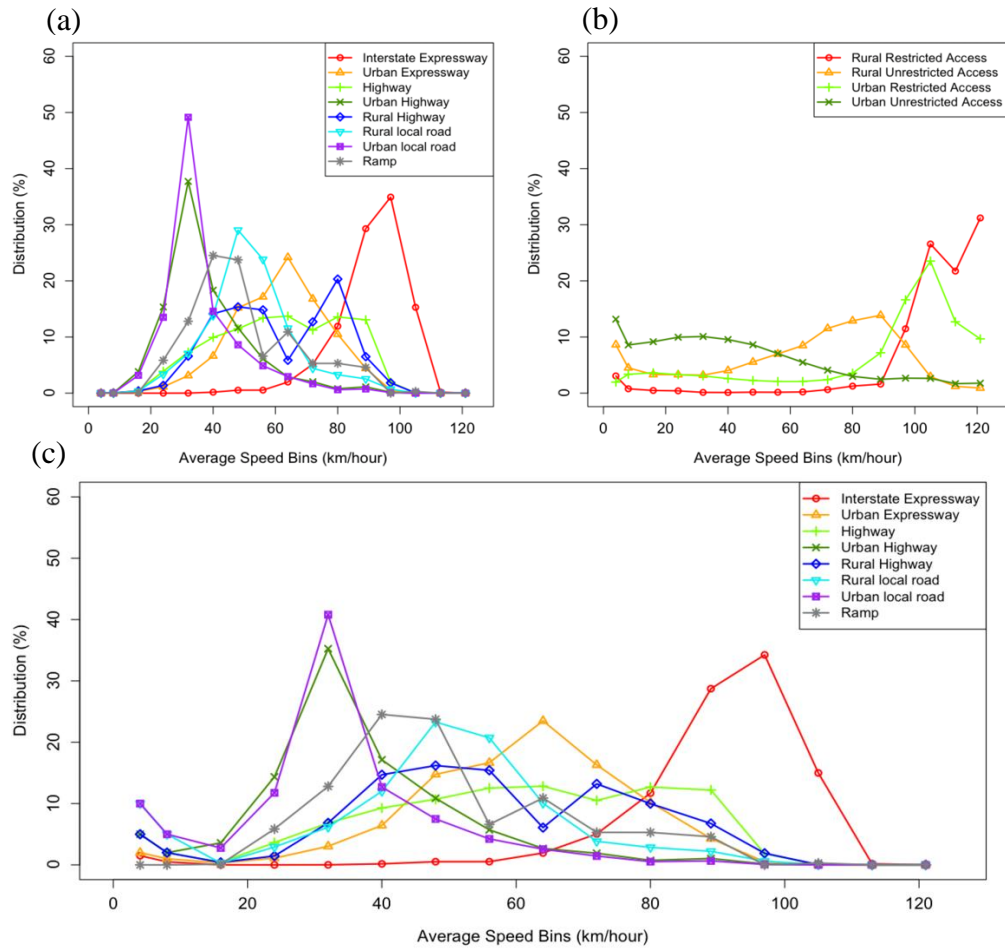
1024



1025

1026 **Figure 3.** Variation of NO_x emission factors from diesel compact engines by vehicle speed and
 1027 ambient temperatures: **(a)** NO_x emission factors function to vehicle speed; **(b)** NO_x emission
 1028 factors of diesel compact truck function to vehicle speed and ambient temperature.

1029



1030

1031

1032

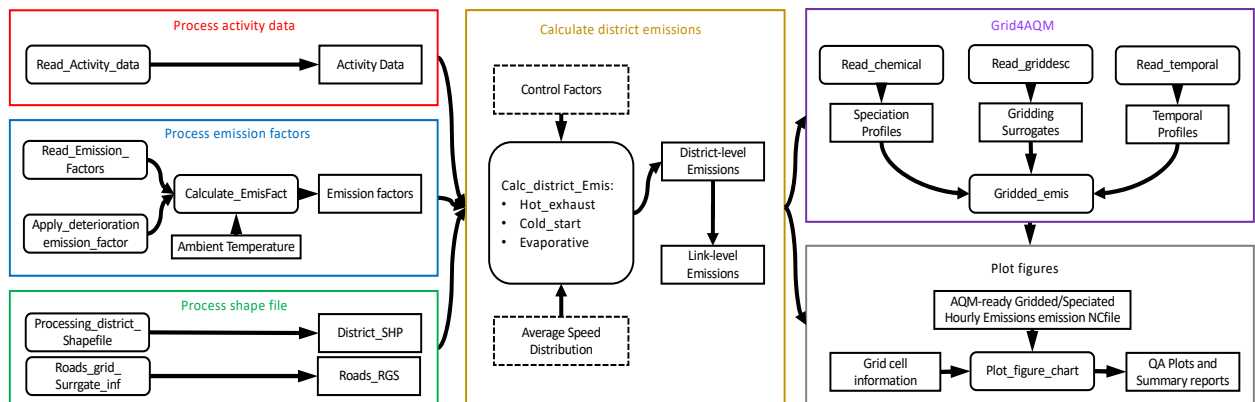
1033

1034

1035

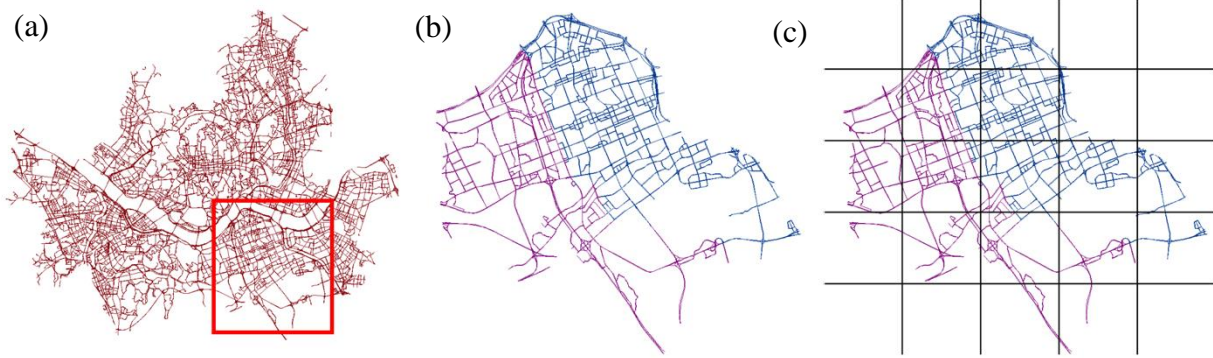
1036

Figure 4. (a) The South Korea speed distribution by road types. (b) The Georgia state speed distribution by road types. (c) The average speed distribution (ASD) by road types used in this study for South Korea.

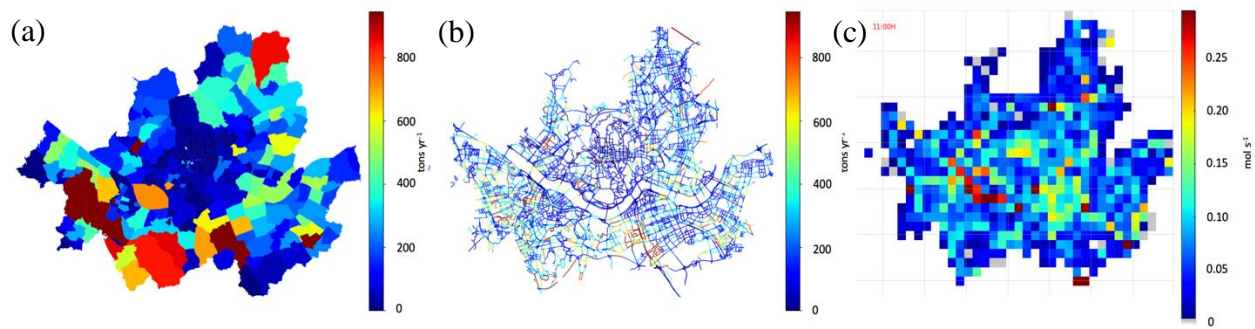


1037
1038
1039

Figure 5. The schematic of modules and their functions in the CARS.



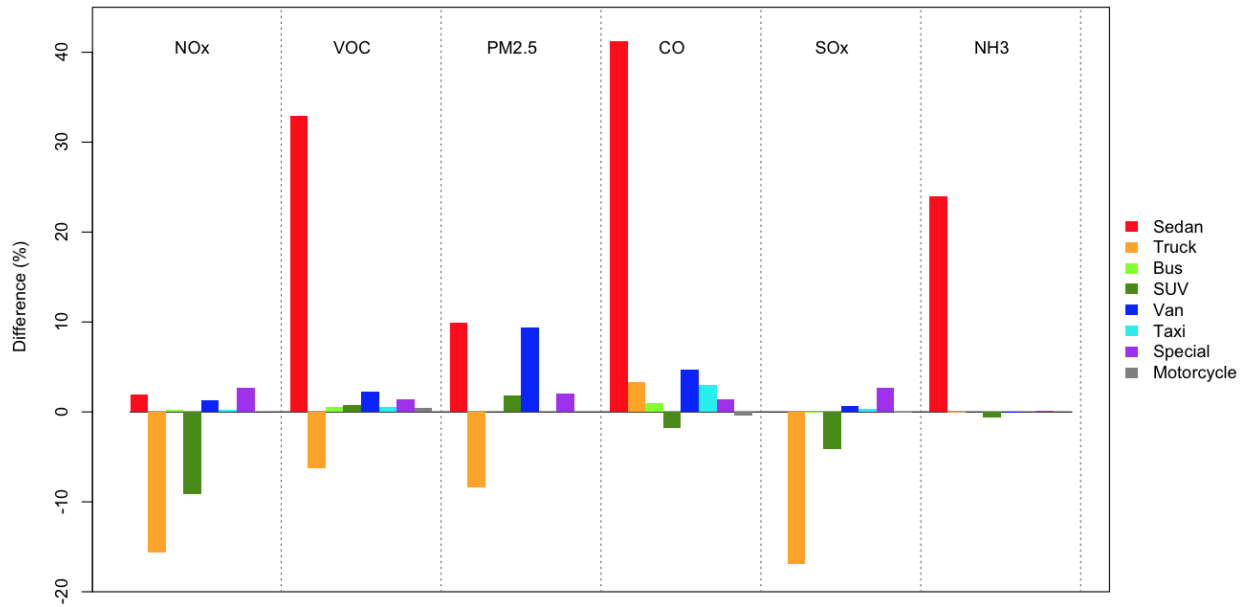
1040
1041 **Figure 6** (a) the road network GIS shapefile of Seoul, South Korea; (b) two districts with different
1042 colors (purple and blue); (c) the modeling grid cells over road segments.
1043



1044

1045 **Figure 7.** Three different formats of CO emissions from CARS, (A) District-level total emissions
 1046 (t yr^{-1}) (B) Link-level total emissions (t yr^{-1}), (C) CTM-ready gridded hourly total emissions (moles
 1047 s^{-1}).

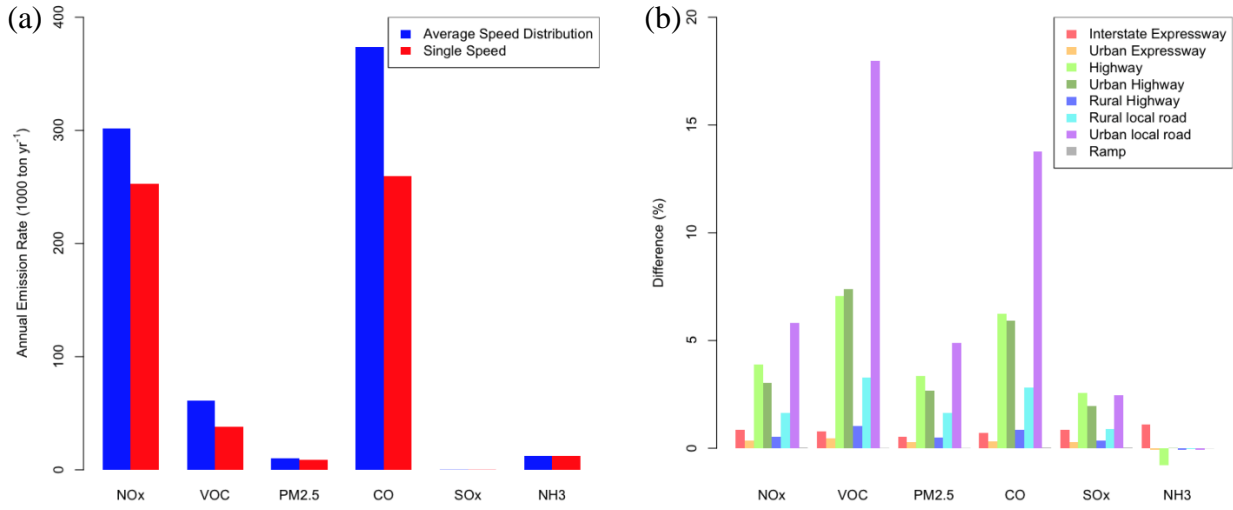
1048



1049
 1050
 1051
 1052

Figure 8. Comparison between CARS 2015 and CAPSS 2015 onroad mobile emissions inventories by vehicle types. The standard line is CAPSS 2015 data.

1053



1054
1055
1056
1057

Figure 9. The impacts of emissions between the ASD and single-speed approach: (a) the total emission differences by pollutant; (b) The road-specific difference (%) by pollutant.

1058 **Appendix**

1059

1060

1061 **Appendix A:** The vehicle types classified by fuel type, vehicle body type, and engine size. The
 1062 emission factors of the diesel vehicle with the star (*) are depended on the ambient temperature
 1063 (*T*).

Vehicle Types	Fuel Types							
	Gasoline	Diesel	LPG	CNG	HYBRID_G	HYBRID_D	HYBRID_L	HYBRID_C
Sedan	Supercompact	Supercompact*	Supercompact	-	-	-	-	-
	Compact	compact*	compact	compact	compact	compact	compact	-
	Fullsize	Fullsize*	Fullsize	Fullsize	Fullsize	Fullsize	Fullsize	-
	Midsize	Midsize*	Midsize	Midsize	Midsize	Midsize	Midsize	-
Truck	Supercompact	Supercompact	Supercompact	-	-	-	-	-
	Compact	Compact*	Compact	Compact	-	-	-	-
	Fullsize	Concrete	-	Fullsize	-	-	-	-
	Midsize	Fullsize	Midsize	Midsize	-	-	-	-
	-	Midsize	-	-	-	-	-	-
	-	Dump	-	-	-	-	-	-
	-	Special	Special	Special	-	-	-	-
Bus	Urban	Urban	Urban	Urban	-	Urban	-	-
	Rural	Rural	Rural	Rural	-	Rural	-	Rural
SUV	Compact	Compact*	Compact	-	-	-	-	-
	Midsize	Midsize*	Midsize	Midsize	Midsize	-	-	-
Van	supercompact	supercompact	supercompact	-	-	-	-	-
	Compact	Compact	Compact	Compact	-	-	-	-
	-	-	Fullsize	Fullsize	Fullsize	Fullsize	Fullsize	Fullsize
	Midsize	Midsize	Midsize	Midsize	Midsize	Midsize	Midsize	Midsize
Taxi	-	-	Compact	-	-	-	-	-
	-	-	Fullsize	-	-	-	-	-
	-	-	Midsize	-	-	-	-	-
Special	-	Tow	-	-	-	-	-	-
	Wrecking	Wrecking	Wrecking	Wrecking	-	-	-	-
	Others	Others	Others	-	-	-	-	-
Motorcycle	Compact	-	-	-	-	-	-	-
	Midsize	-	-	-	-	-	-	-
	Fullsize	-	-	-	-	-	-	-

1064 - no existence

1065 * ambient temperature-dependent diesel vehicle

1066 LPG: Liquefied Petroleum Gas

1067 CNG: Connecticut Natural Gas

1068 Hybrid_G: hybrid vehicle with gasoline

1069 Hybrid_D: hybrid vehicle with diesel

1070 Hybrid_L: hybrid vehicle with LPG

1071 Hybrid_C: hybrid vehicle with CNG

1072

1073

1074 **Appendix B**, The summary of activity data (number of vehicles and daily total VKTs) in South
 1075 Korea by vehicle type with engine size.

Vehicle Types	Engine sizes	Fuel Types									
		Gasoline		Diesel		LPG		CNG		Hybrid	
		Numbers	Daily VKT	Numbers	Daily VKT	Numbers	Daily VKT	Numbers	Daily VKT	Numbers	Daily VKT
Sedan	Supercompact	1,792,471	50,197,345	46	1,761	83,226	4,000,067	6	237	-	-
	Compact	1,372,317	39,543,668	51,324	2,570,086	8,040	257,060	276	12,115	3,802	137,360
	Fullsize	2,403,327	100,632,702	428,831	20,928,552	292,850	15,910,588	5,296	323,852	21,533	1,086,509
	Midsized	4,858,533	167,454,032	672,960	33,126,318	1,431,970	66,640,378	4,310	625,717	140,527	6,717,856
Truck	Supercompact	850	9,595	816	354	111,051	6,550,476	-	-	-	-
	Compact	3,185	143,510	2,655,089	133,480,216	87,650	3,567,109	42	2,694	-	-
	Fullsize	3	422	180,991	25,774,819	-	-	72	4,676	-	-
	Midsized	98	7,430	258,509	17,477,685	1,434	47,870	14	483	-	-
	Dump	-	-	-	-	-	-	-	-	-	-
	Special	20	970	-	-	2,292	99,124	1,194	60,886	-	-
Bus	Urban	1	126	40,448	7,282,593	1	652	6,543	1,466,854	2	282
	Rural	-	-	34,997	6,334,278	-	-	30,792	6,460,001	216	50,873
SUV	Compact	42,348	1,395,153	2,341,397	105,962,626	6,946	275,728	13	551	-	-
	Midsized	91,002	3,520,552	1,120,128	5,277,861	13,567	595,426	15	706	1,719	88,683
Van	supercompact	88	1,645	-	-	44,947	2,058,014	-	-	-	-
	Compact	2,937	87,507	685,317	34,781,937	151,654	6,135,138	7	255	-	-
	Fullsize	-	-	19,452	1,318,221	1	14	97	7,598	3	136
	Midsized	2	1,303,795	31,790	1,433,407	15	416	160	15,216	2	85
	Special	-	-	-	-	-	-	-	-	-	-
Taxi	Compact	-	-	-	-	8,380	576,378	-	-	-	-
	Fullsize	-	-	-	-	92,861	10,827,756	-	-	-	-
	Midsized	-	-	-	-	474,455	69,087,721	-	-	-	-
Special	Tow	-	-	40,807	7,447,773	-	-	-	-	-	-
	Wrecking	2	138	12,568	813,746	128	6,607	3	94	-	-
	Others	47	553	28,275	989,988	180	9,966	-	-	-	-
Motorcycle	Compact	184,822	3,507,948	-	-	-	-	-	-	-	-
	Fullsize	65,964	3,493,728	-	-	-	-	-	-	-	-
	Midsized	1,910,988	61,676,824	-	-	-	-	-	-	-	-

- 1076 - no existence
- 1077 LPG: Liquefied Petroleum Gas
- 1078 CNG: Connecticut Natural Gas
- 1079 Hybrid: all hybrid vehicles, electric power mixed with fossil fuel (gasoline, diesel, LPG, or CNG)
- 1080
- 1081
- 1082

1083

1084 **Appendix C**, Eight road types with assigned average vehicle operating speed and VKT fractions.

Road types	Description	Average Speed (km h ⁻¹)	Road VKT fraction
101	Interstate Expressway	90	41%
102	Urban Expressway	60	5%
103	Highway	58	18%
104	Urban Highway	36	12%
105	Rural Highway	55	3%
106	Rural Local Road	45	4%
107	Urban Local Road	32	17%
108	Ramp	50	0.4%

1085

1086

1087 **Appendix D**, The daily average VKT (km d⁻¹) per vehicle by vehicle and fuel types.

Vehicle types	Fuel Types					
	Gasoline	Diesel	LPG	CNG	Hybrid	Average
Sedan	34	49	48	97	48	38
Truck	39	57	51	52	-	57
Bus	126	180	-	212	237	191
SUV	37	46	42	45	52	46
VAN	29	51	42	87	44	49
Taxi	-	-	140	-	-	140
Special	14	113	54	31	-	113
Motorcycle	32	-	-	-	-	32

1088

1089

1090 **Appendix E**, Average speed distribution (ASD) for each road type: The table columns are
 1091 different road types, and the table rows are average speed of each speed bin.

Speed bins	Speed (km/h)	Road Types							
		101	102	103	104	105	106	107	108
1	speed < 4	1.50%	2.00%	5.00%	5.00%	5.00%	10.00%	10.00%	0.00%
2	4 ≤ speed < 8	0.50%	1.00%	2.00%	2.00%	2.00%	5.00%	5.00%	0.00%
3	8 ≤ speed < 16	0.00%	0.33%	0.40%	3.59%	0.41%	0.30%	2.76%	0.11%
4	16 ≤ speed < 24	0.00%	1.09%	3.64%	14.35%	1.45%	2.91%	11.75%	5.85%
5	24 ≤ speed < 32	0.01%	3.04%	6.82%	35.25%	6.85%	6.15%	40.80%	12.80%
6	32 ≤ speed < 40	0.17%	6.43%	9.28%	17.14%	14.70%	12.00%	12.69%	24.53%
7	40 ≤ speed < 48	0.52%	14.76%	10.70%	10.86%	16.20%	23.30%	7.49%	23.74%
8	48 ≤ speed < 56	0.53%	16.66%	12.52%	5.72%	15.42%	20.72%	4.24%	6.60%
9	56 ≤ speed < 64	1.94%	23.49%	12.83%	2.68%	6.08%	10.06%	2.56%	10.90%
10	64 ≤ speed < 72	5.05%	16.30%	10.51%	1.90%	13.21%	3.84%	1.45%	5.30%
11	72 ≤ speed < 80	11.70%	10.19%	12.69%	0.74%	9.98%	2.85%	0.53%	5.30%
12	80 ≤ speed < 89	28.73%	4.30%	12.21%	1.04%	6.75%	2.21%	0.65%	4.59%
13	89 ≤ speed < 97	34.24%	0.51%	1.82%	0.15%	1.90%	0.62%	0.08%	0.00%
14	97 ≤ speed < 105	14.99%	0.00%	0.02%	0.00%	0.04%	0.03%	0.00%	0.30%
15	105 ≤ speed < 113	0.18%	0.00%	0.00%	0.00%	0.00%	0.00%	0.00%	0.00%
16	113 ≤ speed < 121	0.01%	0.00%	0.00%	0.00%	0.00%	0.00%	0.00%	0.00%

1092 **Appendix F**: Single average speed for each road type

Speed bins	Speed (km/h)	Road Types							
		101	102	103	104	105	106	107	108
1	speed < 4	0%	0%	0%	0%	0%	0%	0%	0%
2	4 ≤ speed < 8	0%	0%	0%	0%	0%	0%	0%	0%
3	8 ≤ speed < 16	0%	0%	0%	0%	0%	0%	0%	0%
4	16 ≤ speed < 24	0%	0%	0%	0%	0%	0%	0%	0%
5	24 ≤ speed < 32	0%	0%	0%	0%	0%	0%	100%	0%
6	32 ≤ speed < 40	0%	0%	0%	100%	0%	0%	0%	0%
7	40 ≤ speed < 48	0%	0%	0%	0%	0%	100%	0%	100%
8	48 ≤ speed < 56	0%	0%	100%	0%	100%	0%	0%	0%
9	56 ≤ speed < 64	0%	100%	0%	0%	0%	0%	0%	0%
10	64 ≤ speed < 72	0%	0%	0%	0%	0%	0%	0%	0%
11	72 ≤ speed < 80	0%	0%	0%	0%	0%	0%	0%	0%
12	80 ≤ speed < 89	100%	0%	0%	0%	0%	0%	0%	0%
13	89 ≤ speed < 97	0%	0%	0%	0%	0%	0%	0%	0%
14	97 ≤ speed < 105	0%	0%	0%	0%	0%	0%	0%	0%
15	105 ≤ speed < 113	0%	0%	0%	0%	0%	0%	0%	0%
16	113 ≤ speed < 121	0%	0%	0%	0%	0%	0%	0%	0%

1093

1094 **Appendix G:**

1095

1096 The annual emission rate between original road type ASD, adjusted road type ASD, and CAPSS
 1097 result for 2015

Gg/year	CO	NOx	SOx	PM10	PM2.5	VOC	NH3
CARS data 2015 org ASD	269.3	258.4	0.2	9.5	8.8	38.9	12.4
CARS data 2015 adj ASD	373.9	301.8	0.2	11.0	10.1	61.2	12.5
CAPSS 2015	245.5	369.6	0.2	9.6	8.8	46.1	10.1

1098

1099

1100

1101 **Appendix H:**

1102

1103 CARS model input data summary table

Input data type	Parameters	Variable Name in CARS	File format
Human activity data of each vehicle	Fuel, vehicle, type, daily VKT, region code, manufacture data	activity_file	csv
Emission factor table	Vehicle, engine, fuel, SCC ,Pollutant, year, temperature, v,a,b,c,d,f,k	Emis_factor_list	csv
Link level Shape file	Link ID, region code, region name, road rank, speed, VKT, Link length, geometry	Link_shape	shape file
County Shape File	Region code, region name	county_shape	shape file
Average speed distribution table	Speed bins, the distribution of each road type	avg_SPD_Dist_file	csv
road restriction table	Vehicle, engine, fuel, road types	road_restriction	csv
Vehicle deterioration table	Vehicle, engine, SCC, fuel, Pollutant, Manufacture date	Deterioration_list	csv
Control strategy factors table	Vehicle, engine, fuel, year, data, region code, control factor	control_list	csv
Model domain description	Projection method name, parameters for prjection method, domain name, bottum left coner X and Y, grid cell size, numbers of grid cell in X, Y, and Z-axis	gridfile_name	text file in griddesc format
Temporal profile tables	Profile reference number, Year to Monthly profile (12 columns)	temporal _monthly_file	csv
	Profile reference number, week to daily profile (7 columns)	temporal _week_file	csv

	Profile reference number, week day to hourly profile (24 columns)	temporal_weekday_file	csv
	Profile reference number, weekend day to hourly profile (24 columns)	temporal_weekend_file	csv
	Vehicle, types, fuel, road type, month reference number, week reference number, weekday reference number, weekend reference number	temporal_CrossRef	csv
Chemical profile table	Species code, species name, target species name, fraction, molecular weight,	Chemical_profile	txt or csv
	Vehicle, engine, fuel, species reference codes	speciation_CrossRef	csv

1104
1105